

CRITERIA FOR NUMERICAL STABILITY  
OF ELASTIC-VISCOPLASTICITY

CRITERIA FOR NUMERICAL STABILITY OF  
EXPLICIT TIME-STEPPING  
ELASTIC-VISCOPLASTICITY

By

JERRY EARL HIGGINS, B.ENG.

A Thesis

Submitted to the School of Graduate Studies  
in Partial Fulfilment of the Requirements  
for the Degree  
Master of Engineering

McMaster University

(c) Copyright by Jerry Earl Higgins, June 1989

McMASTER UNIVERSITY LIBRARY

MASTER OF ENGINEERING (1989)  
(Civil Engineering)

McMASTER UNIVERSITY  
Hamilton, Ontario

TITLE:                   Criteria For Numerical Stability  
                          of Explicit Time-Stepping  
                          Elastic-Viscoplasticity

AUTHOR:                 Jerry Earl Higgins, B.ENG.  
                          (McMaster University)

SUPERVISOR:            Dr. D.F.E. Stolle

NUMBER OF PAGES: xv,95

## ABSTRACT

A simple yet effective technique is used to obtain a numerical stability criteria for explicit time-marching algorithms in elastic-viscoplasticity. The resulting stability criteria are capable of accounting for non-associative and work hardening viscoplasticity for a wide variety of constitutive laws of the Perzyna-type. Conservative estimates for maximum permissible time step are obtained. This thesis investigates the level of conservativeness by considering different problems exhibiting various levels of constraint. Using the proposed stability criterion, assuming a linear flow function, non-hardening and uniform material properties, it is shown that the initial strain algorithm for plasticity and the initial strain viscoplastic algorithms are numerically the same. The intuitive approach used to obtain an estimate of maximum permissible time step was also used to develop an unconditionally stable implicit time marching scheme which avoids expensive matrix inversions.

## ACKNOWLEDGEMENTS

I would like to express my sincerest gratitude to the following individuals who assisted in the research and preparation of this thesis.

For his intellectual criticism, proofreading, guidance and encouragement, I am indebted to my supervisor, Dr. Dieter Stolle.

Financial support of Dr. D. Stolle and McMaster University is gratefully acknowledged.

Note of thanks to Mr. Peter Koudys for his general helpfulness throughout my involvement at McMaster university.

To my mother and father and other members of my family for supporting me in my endeavours.

Finally, I would like to thank my wife, Roxanne, for providing her love and sacrifice when it was needed most.

## TABLE OF CONTENTS

	Page
ABSTRACT	iii
ACKNOWLEDGEMENTS	iv
TABLE OF CONTENTS	v
LIST OF FIGURES	viii
LIST OF SYMBOLS	x
CHAPTER 1 INTRODUCTION	1
1.1 General	1
1.2 Objective and Scope	4
CHAPTER 2 ELASTIC/VISCOPLASTICITY	6
2.1 Elastic/Viscoplastic Theory	6
2.2 Yield Criterion	8
2.2.1 Drucker-Prager Material	9
2.2.2 Mohr-Coulomb Material	10
2.2.3 Simplifications for Two-Dimensional Problems	12
CHAPTER 3 NON-LINEAR FINITE ELEMENT FORMULATION	17
3.1 General Non-Linear Finite Element Formulation	15
3.2 Elastic/Viscoplastic Implementation for Plasticity	19
3.3 Overview	21
CHAPTER 4 NUMERICAL STABILITY IN VISCOPLASTICITY	22

TABLE OF CONTENTS (continued)

	4.1 General	22
	4.2 Literature Review Viscoplastic Numerical Stability	23
	4.3 Numerical Stability for One Dimensional Problems	25
	4.4 Traditional Approach for Numerical Stability	28
	4.5 Proposed Approach for a Numerical Stability Criterion	30
	4.6 Examples of Numerical Stability Criterion Expression	33
CHAPTER	5 ELASTIC AND VISCOPLASTIC FINITE ELEMENT SIMULATIONS	38
	5.1 Introduction	38
	5.2 Comparison with Steady State Creep and Elasticity	38
	5.3 Numerical Instability Associated with Creep Problems	40
	5.3.1 Stress Relaxation Problems	41
	5.3.2 Creep of a Thick-Walled Cylinder - Instability	46
	5.4 Elastic/Viscoplastic Instability	47
CHAPTER	6 ANALYSIS OF PLASTICITY PROBLEMS	66
	6.1 Plasticity Solutions via a Viscoplastic Approach	66
	6.2 Plasticity Examples	68
	6.2.1 Thick-Walled Cylinder	69

TABLE OF CONTENTS (continued)

6.2.2	Strip Footing Problem	71
6.3	Summary of Examples	72
CHAPTER	7 CONCLUSIONS AND RECOMMENDATIONS	76
7.1	Conclusions	77
7.2	Recommendations	79
APPENDIX	A AN IMPLICIT VISCOPLASTIC FORMULATION	80
APPENDIX	B NUMERICAL STABILITY OF DEVIATORIC AND VOLUMETRIC HARDENING MODELS	82
	B.1 General	82
	B.1.1 Deviatoric Model	82
	B.1.2 Volumetric Model	84
APPENDIX	C DERIVATION DETAILS OF NUMERICAL STABILITY EXPRESSIONS	86
	C.1 General	86
	C.1.1 Numerical Stability for Mohr-Coulomb Yield Description	86
	C.1.2 Numerical Stability for a von-Mises Yield Description	88
APPENDIX	D CLOSED FORM 1-D STABILITY CRITERION	90
REFERENCES		92

## LIST OF FIGURES

Figure	Page
2.1 Elastic-Plastic/Viscoplastic Response	14
2.2 Drucker-Prager and von Mises Yield Description	15
2.3 Mohr-Coulomb and Tresca Yield Description	15
2.4 Mohr-Coulomb Two-Dimensional Yield Description	16
4.1 One-Dimensional Constant Stress Creep Configuration	35
4.2 One-Dimensional Constant Strain Creep Configuration	35
4.3 One-Dimensional Instability Demonstration : $m = 1$	36
4.4 One-Dimensional Instability Demonstration : $m = 3$	37
5.1 Plane Strain Strip Footing - 70 Element Grid	51
5.2 Vertical Stress Profile - Plane Strain Strip Footing	52
5.3 Horizontal Stress Profile - Plane Strain Strip Footing	53
5.4 Shear Stress Profile - Plane Strain Strip Footing	54
5.5 Axisymmetric Thick-Walled Cylinder - 10 Element Grid	55
5.6 Axisymmetric Thick-Walled Cylinder Elastic and Steady State Creep Solution	56
5.7 Stress Relaxation - 1 Element Grid	57
5.8 Instability Demonstration for Pure Stress Relaxation $\Delta\epsilon_a = \Delta\epsilon_r = \Delta\epsilon_\theta = 0$ : $m = 1$	58
5.9 Instability Demonstration for Pure Stress Relaxation $\Delta\epsilon_a = \Delta\epsilon_r = \Delta\epsilon_\theta = 0$ : $m = 3$	59

### LIST OF FIGURES (Continued)

5.10	Instability Demonstration for Stress Relaxation $\Delta\varepsilon_r \neq 0 : m = 1$	60
5.11	Instability Demonstration for Stress Relaxation $\Delta\varepsilon_r \neq 0 : m = 3$	61
5.12	Instability Demonstration : $m = 1$ Creep of Axisymmetric Thick Walled Cylinder	62
5.13	Instability Demonstration : $m = 3$ Creep of Axisymmetric Thick Walled Cylinder	63
5.14	Instability Demonstration Stress Relaxation : Mohr-Coulomb Plane Strain	64
5.15	Level of Conservativeness Demonstrated Stress Relaxation : Mohr-Coulomb Plane Strain	65
6.1	Progression of Plastic Zones : Instability Axisymmetric Thick-Walled Cylinder - Tresca	74
6.2	Surface Displacement at Centre of Strip Footing Plane Strain Tresca - Instability Explored	75
6.3	Stress Oscillations beneath centre of Strip Footing Tresca - 10th Load Increment : Yield = -40 kPa	76

## LIST OF SYMBOLS

a	strip footing width in metres
$a_0$	critical state major elliptic axis length
$\Delta a_n$	nodal displacement increment vector at $t_n$
$a_n$	vector containing nodal displacements at $t_n$
$b_n$	vector containing body forces
c	material cohesion
$c_i$	yielded radii of thick-walled cylinder
e	displacement based error in non-linear solution
$e_{max}$	maximum tolerance governing convergence
$f(\Sigma)$	system of nonlinear functions of $\Sigma$
$f(\Sigma_n)$	system of nonlinear functions of $\Sigma_n$
m	power law exponent
$p_0$	reference for deviatoric model along p-axis
$p_i$	inner stress applied to a thick-walled cylinder
p	$= (\sigma_{11} + \sigma_{22})$ stress parameters
q	$= [(\sigma_{11} - \sigma_{22})^2 + 4(\sigma_{12})^2]^{1/2}$ for plane strain or axial symmetry
$q_f$	$= 5.14c$ ; solution for strip footing failure
r	radial location within thick-walled cylinder
$r_i$	inner radii of thick-walled cylinder
$r_o$	outer radii of thick-walled cylinder
$s_{ij}$	stress deviator components
$\Delta t_n$	time increment corresponding to $t_{n+1} - t_n$

LIST OF SYMBOLS (Continued)

$\Delta t_{\text{crit}}$	estimate of maximum time step representing stable oscillatory behaviour
$\Delta t_{\text{crit}}^{1D}$	stable oscillatory maximum time step for one dimension
$\Delta t_{\text{max}}$	non-oscillatory maximum time step based on changes in $\Gamma$ or for one dimension
$\Delta t_{\text{max}}^F$	non-oscillatory maximum time step based on changes in $F$
$\Delta t_{\text{max}}^{1D}$	non-oscillatory maximum time step for one dimension
$u_y$	surface displacements under strip footing
$u_n$	vector containing displacements at time, $t_n$
$\delta u$	arbitrary virtual displacement
$\delta u_n$	arbitrary virtual displacement at time, $t_n$
$A$	viscoplastic or creep strain fluidity parameter
$B$	kinematic matrix relating strains to displacements
$C$	$= f(\Sigma_n) - J_n \Sigma_n$ ; represents a constant
$D^{VP}$	tangent matrix
$D$	material matrix
$E_1$	$= E(1-\nu)/[(1+\nu)(1-2\nu)]$
$E$	elastic modulus
$F$	static yield surface function
$H_e$	$= (\partial F/\partial \sigma)^T D (\partial Q/\partial \sigma)$ ; elastic hardening parameter
$H_p$	viscoplastic hardening parameter

LIST OF SYMBOLS (Continued)

I	identity matrix
$I_1$	first stress invariant
$J_2'$	second deviatoric stress invariant
$J_3'$	third deviatoric stress invariant
J	Jacobian matrix of f
$J_n$	Jacobian matrix of f at time, $t_n$
K	$= \frac{6c \cos \phi}{3^{1/2} (3 - \sin \phi)}$ Material constant used in Drucker-Prager yield description
L	material parameter used in the deviatoric model
M	$= 1 + \Gamma' \Delta t_n (H_e + H_p)$ ; used in implicit formulation
N	matrix containing the element shape functions
$Q_1$	plastic potential surface intersecting $\sigma^e$
$Q_2$	plastic potential surface intersecting F
$R_n$	applied loads at time, $t_n$
$R_{n+1}$	$= R_n + \Delta R_n$ ; applied loads at time, $t_{n+1}$
$\Delta R_n$	applied loads increment at time, $t_n$
S	surface of body
$T_n$	vector containing boundary tractions
V	volume of body
Y	$= 2c$ ; yield stress for von mises criterion
$\alpha$	$= \frac{2 \sin \phi}{3^{1/2} (3 - \sin \phi)}$ Material constant used in Drucker-Prager yield description

LIST OF SYMBOLS (Continued)

$B$	plastic strain rate proportionality constant
$\delta_{ij}$	Kronecker Delta ; $\delta_{ij}=1$ if $i=j$ and $\delta_{ij}=0$ if $i \neq j$ .
$\Delta\delta_j$	$j$ th degree of freedom displacement increment
$\epsilon$	uniaxial total strain
$\dot{\epsilon}$	uniaxial total strain rate
$\dot{\epsilon}^c$	uniaxial creep strain rate
$\epsilon_n$	uniaxial total strain at time, $t_n$
$\epsilon_{n+1}$	uniaxial total strain at time, $t_{n+1}$
$\delta\epsilon_n$	arbitrary virtual strain vector at time, $t_n$
$\epsilon$	total strain vector
$\epsilon_{ij}$	total strain vector components
$\epsilon^e$	elastic strain vector
$\epsilon^p$	plastic strain vector
$\epsilon^{vp}$	viscoplastic strain vector
$\dot{\epsilon}^{vp}$	viscoplastic strain rate vector
$\dot{\epsilon}_{ij}^{vp}$	viscoplastic strain rate vector components
$\epsilon_q^p$	plastic deviatoric strain
$\epsilon_v^p$	plastic volumetric strain
$\epsilon_n$	vector containing total strains at time, $t_n$
$\Delta\epsilon_n$	total strain increment vector at time, $t_n$
$\Delta\epsilon_{ij}$	total strain increment vector components
$\Delta\epsilon_{ij}^e$	elastic strain increment vector components

LIST OF SYMBOLS (Continued)

$\Delta\epsilon_{ij}^{vp}$	viscoplastic strain increment vector components
$\Delta\epsilon^p$	plastic strain increment vector
$\dot{\sigma}$	uniaxial stress rate
$\sigma$	uniaxial stress
$\sigma_0$	initial uniaxial state of stress
$\sigma_n$	uniaxial state of stress at time, $t_n$
$\sigma$	vector containing stresses
$\sigma_{ij}$	stress vector components
$\sigma_n$	vector containing stresses at time, $t_n$
$\sigma_{n+1}$	$=\sigma_n + \Delta\sigma_n$ ; stress vector at time, $t_{n+1}$
$\Delta\sigma_n$	stress increment vector at time, $t_n$
$\sigma_0$	initial state of stress vector
$\sigma^e$	$=\sigma_0 + D \Delta\epsilon$ ; fictitious stress used to evaluate $\beta$
$\sigma_n^\dagger$	$=\sigma_n - D \Delta\epsilon_n^{vp}$ ; initial stress level used in the initial strain viscoplastic approach
$\sigma_e$	$=(3J_2')^{1/2}$ effective stress
$\sigma_a$	axial stress component
$\sigma_r$	radial stress component
$\sigma_\theta$	tangent stress component
$\sigma_x$	horizontal stress component; plane strain
$\sigma_y$	vertical stress component; plane strain
$\eta_f$	represents stress ratio $q/p$ at failure state

LIST OF SYMBOLS (Continued)

$\eta_c$	represents ratio $q/p$ at zero dilatancy state
$\eta(\epsilon_q^p)$	$= \eta_f \frac{\epsilon_q^p}{L + \epsilon_q^p}$ hyperbolic function of deviatoric plastic strains
$\phi$	static friction angle of material modelled
$\psi$	dynamic friction angle of material modelled
$\theta$	represents an angle in the $\pi$ -plane
$\nu$	Poisson's ratio
$\mu$	$= -EA$
$\lambda_{max}$	largest eigenvalue of the Jacobian matrix $J$
$\kappa$	represents a hardening parameter
$\Gamma$	viscoplastic strain rate proportionality function
$\Gamma'$	$= \partial\Gamma / \partial F$
$\phi(F)$	flow function
$\Sigma$	vector containing stresses at all integration points
$\Sigma_n$	vector containing stresses at all integration points at time, $t_n$
$\Psi_{n+1}$	equilibrium expression at time, $t_{n+1}$
$\Psi_n$	equilibrium expression at time $t_n$

CHAPTER 1  
INTRODUCTION

1.1 General

Since the early 1970's, much research has been carried out on elastic-viscoplastic modelling of problems in geomechanics using the finite element method. In elastic-viscoplasticity, we have in addition to reversible elastic strains,  $\epsilon^e$ , an additional set of viscoplastic strains,  $\epsilon^{vp}$ . These time-dependent strains are characterized by a strain rate which is zero when stresses are below a certain threshold (or yield) value and exhibit a finite strain rate only when this threshold is exceeded [1].

Elastic-Viscoplastic modelling has been used extensively, both, as a means to predict the transient response associated with creep, and as an alternative numerical procedure for obtaining solutions to plasticity problems [1-10]. The advantages of dealing with plasticity, creep and viscoplasticity in a unified manner are discussed in Reference [1]. In particular, it is suggested that the use of the elastic-viscoplastic approach is advantageous for the treatment of non-associated plasticity and strain softening situations which may be difficult to implement when using a

conventional plasticity approach [1]. The fact that a wide variety of materially non-linear problems can be treated within a standard programme is also an advantage.

The elastic-viscoplastic approach has been used to solve a wide variety of problems in geomechanics, including: the analysis of tunnels in soil or rock, taking into account excavation and/or gravity loading [1,9,11,12]; strip loaded homogeneous and layered soils [9,11]; and excavation and gravity loading associated with homogeneous and layered soil embankments [9,11]. Viscoplastic modelling applications have been extended to include large deformations [2,6,10], development of complex viscoplastic constitutive equations involving isotropic and kinematic hardening for cyclic loading [13], and the prediction of creep crack growth using a viscoplastic continuum damage concept [14].

The application of elastic-viscoplastic modelling for various numerical solution techniques, other than the finite element method, has also been considered. The traditional finite element procedure has been extended to include infinite/semi-infinite domain via an infinite finite element method [11] and in more recent years, elastic-viscoplastic constitutive models have been incorporated into boundary element codes [7].

Owing to the nature of elastic-viscoplasticity problems, the analyses require time integration algorithms for

obtaining solutions to boundary-value problems. When using viscoplasticity algorithms to solve plasticity problems the time-stepping replaces the iteration loop which is used in the classical plasticity algorithms. Much research has been done in the past for determining appropriate algorithms for solving viscoplasticity problems. Since computer costs associated with such modelling may be considerable, research in the past has addressed the problem of minimizing the computational effort by maximizing the time step. This has been achieved by obtaining theoretical upper bounds on time steps for explicit, Euler-type algorithms [1,7,15-17] and developing unconditionally stable implicit [2,8,14,17-19] and implicit-explicit [11,14] time marching schemes. The efficiency of a specific method depends on boundary conditions and the degree of material non-linearity [20].

Analyses dealing with viscoplasticity are generally completed using explicit or implicit schemes. The implicit-explicit technique which is a combination of implicit and explicit strategies is a relatively new development. The basic idea is to combine the lesser expensive, but conditionally stable, explicit time integration with the more stable, but computationally more costly, implicit rule [11]. In boundary-value problems where non-homogeneous material exists or where part of the domain is subjected to significantly higher values of stress when compared with yield

limits, the time step limits throughout the domain can be considerably different [11,14]. In such cases the domain is divided into appropriate implicit and explicit regions. In this way larger time step lengths can be used and expensive implicit integration of the "entire" finite element mesh is avoided.

The key to the success of explicit, or implicit-explicit schemes is in the ability to estimate realistic maximum allowable time steps which ensure a stable numerical response. The study reported herein addresses this specific aspect of viscoplastic modelling.

## 1.2 Objectives and Scope

The main objective of this thesis is to extend Cormeau's work on numerical stability of explicit algorithms in Reference [15] in order to develop a criterion capable of taking into account work hardening and non-associative viscoplasticity in a simple but effective manner. It is assumed in this thesis that numerical stability means the ability to converge, Irons and Ahmad, [21]. An implicit time marching scheme is developed following the same intuitive approach adopted for developing a general stability criteria for providing an estimate of the maximum permissible time step. A direct comparison is also made between viscoplasticity and initial strain plasticity algorithms.

The finite element method is used for all examples shown herein.

Chapters 2, 3 and 4 contain brief theoretical details relevant to this thesis. In particular, in chapter 2, elastic-viscoplastic theory is briefly reviewed and compared with conventional plasticity. Chapter 3 contains details of the non-linear finite element approach adopted in this thesis. Chapter 4, which emphasizes numerical stability, reviews existing approaches and presents a derivation of the criteria used in this thesis. Chapter 5 and 6 demonstrate the application of the stability criteria to elastic-viscoplastic and elastoplastic problems, respectively. In both of these chapters, sensitivity analyses are completed to study the effect of level of constraint and time step length on numerical predictions.

## CHAPTER 2

### A REVIEW ON ELASTIC-VISCOPLASTICITY

#### 2.1 Elastic-Viscoplastic Theory

In elastic/viscoplastic analysis, as presented by Perzyna [22], it is assumed that a body initially undergoes an instantaneous elastic response, followed by the development of time-dependent irrecoverable strains in regions of the body where the stress levels exceed yield conditions. Perzyna suggested that the viscoplastic strain rate  $\dot{\epsilon}^{VP} = \langle \dot{\epsilon}_{11}^{VP}, \dot{\epsilon}_{22}^{VP}, \dot{\epsilon}_{33}^{VP}, \dot{\epsilon}_{12}^{VP}, \dot{\epsilon}_{13}^{VP}, \dot{\epsilon}_{23}^{VP} \rangle^T$  may be given by

$$\dot{\epsilon}^{VP} = A \langle \phi(F) \rangle \frac{\partial Q}{\partial \sigma} \quad (2.1)$$

where  $\sigma = \langle \sigma_{11}, \sigma_{22}, \sigma_{33}, \sigma_{12}, \sigma_{13}, \sigma_{23} \rangle^T$  represents a stress vector,  $\langle \phi(F) \rangle$  is a flow function such that

$$\langle \phi(F) \rangle = \begin{cases} \phi(F) & \text{for } F \geq 0 \\ 0 & \text{for } F < 0, \end{cases} \quad (2.2)$$

$Q$  is a plastic potential function and  $A$  is a fluidity

parameter which is often assumed to be a constant. For the case where  $Q=F$ , such a condition leads to what is generally referred to as an "associative" flow rule.

Figure 2.1 gives a geometric interpretation of Equation 2.1 and compares the viscoplastic strain rate components with those of plasticity. Let us consider the case in which the initial state of stress is given by  $\sigma_0$  as shown in the figure. It is assumed that the initial state of stress is within the elastic domain; i.e.,  $F < 0$ . The static yield surface  $F=0$ , which provides a boundary to the elastic domain, is a function of stresses  $\sigma$ , and some hardening function which usually depends on some measure of viscoplastic strains. For a stress point located at  $\sigma^e = \sigma_0 + \Delta\sigma^e$  and  $F > 0$ , the material begins to yield in an elastic-viscoplastic manner. The strain rate magnitude depends on the distance, which is reflected by the value of  $F$ , between the static surface and the stress point which lies on a dynamic surface. The direction of viscoplastic strain rate is represented by the flow vector  $\partial Q_2 / \partial \sigma$ , which is normal to the plastic potential  $Q_2$ , at the stress point  $\sigma^e$ . It should be noted that in plasticity, the direction of plastic strain is normal to a plastic potential surface,  $Q_1$ , which intersects the static yield surface as shown in Figure 2.1. Although the flow vector for viscoplasticity is not identical to that for plasticity, the difference between the two is usually negligible. It is for

for this reason that viscoplasticity algorithms for solving plasticity problems have been successful.

Flow functions that are used for viscoplastic modelling, are usually based on the power law and exponential creep approximations, [9,22]

$$\phi = F^m \quad (2.3)$$

$$\phi = e^{F-1} \quad (2.4)$$

where  $m$  is a material parameter. The power law form given by Equation 2.3 has been used for the viscoplastic simulations presented in this thesis. For more details on viscoplastic theory, the reader is referred to the comprehensive study completed by Perzyna [22] in 1966. Extensions to Perzyna's work can be found in References [23,24].

## 2.2 Yield Criterion

Various static yield criteria and plastic potential functions can be incorporated into Perzyna's [22] theory for viscoplasticity to more realistically model a material's stress-strain-time behaviour. As expected, the choice of functions depends on the behaviour of the particular material to be modelled.

For the case of an isotropic material it is convenient to express the yield and plastic potential functions in terms of the three stress invariants  $I_1, J_2', J_3'$  given by

$$I_1 = \sigma_{ii} \quad (2.5)$$

$$J_2' = 1/2 s_{ij} s_{ij} \quad (2.6)$$

$$J_3' = s_{ij} s_{jk} s_{kl} \quad (2.7)$$

where  $I_1$  denotes the first stress invariant of the stress tensor  $\sigma_{ij}$ ,  $J_2'$  and  $J_3'$  are the second and third invariant of the stress deviator  $s_{ij} = (\sigma_{ij} - \delta_{ij} I_1 / 3)$  respectively. It is assumed that tension is positive and that repeated indices imply summation.  $\delta_{ij}$  represents the Kronecker Delta where  $\delta_{ij}=1$  if  $i=j$  and  $\delta_{ij}=0$  if  $i \neq j$ .

### 2.2.1 Drucker-Prager Material

The Drucker-Prager yield function [25] is defined by

$$F = \alpha I_1 + J_2'^{1/2} - K \quad (2.8)$$

where  $\alpha = \frac{2 \sin \phi}{3^{1/2} (3 - \sin \phi)}$  and  $K = \frac{6c \cos \phi}{3^{1/2} (3 - \sin \phi)}$

As shown in Figure 2.2, this surface represents a right cylindrical cone in the principal stress space. For a non-hardening model,  $\phi$  and  $c$  represent the friction angle and cohesion, respectively. When a strain hardening material is modelled, both  $\alpha$  and  $K$  are usually assumed to be functions of viscoplastic strain invariants. For the case of  $\phi = 0$ , Equation (2.8) reduces to the von Mises criterion

$$F = (3J_2')^{1/2} - 2c = 0 \quad (2.9)$$

which is represented by the right circular cylinder as shown in Figure 2.2. If the cohesion  $c$ , for a von Mises material, is zero the viscoplastic model reduces to a creep model which implies that a material creeps as long as  $s_{ij} \neq 0$ . Several examples on creep are presented in Chapter 5.

In the von Mises description, the inelastic material response is assumed to be incompressible and independent of hydrostatic stress. Furthermore, the viscoplastic strain rates are coincident with principal stress directions.

### 2.2.2 Mohr-Coulomb Material

The generalized Mohr-Coulomb [26,27] criterion shown geometrically in Figure 2.3 can be expressed in the invariant form as follows:

$$F = I_1/3 \sin \phi + J_2'^{1/2} (\cos \theta - \sin \theta \sin \phi) - c \cos \phi = 0 \quad (2.10)$$

where  $\theta$ , sometimes referred to as the "Lode angle" [27], represents an angle in the  $\pi$ -plane which is given by

$$\sin 3\theta = - \frac{3(3)^{1/2} J_3'}{2(J_2')^{3/2}} \quad (2.11)$$

where  $-\pi/6 < \theta < \pi/6$ . For the case of  $\phi=0$ , Equation (2.10) reduces to the Tresca yield criterion, as shown in Figure 2.3, which is expressed as follows:

$$F = 2 J_2'^{1/2} \cos \theta - 2 c = 0 \quad (2.12)$$

Similar to the von Mises criterion, the Tresca criterion assumes that yielding is independent of the hydrostatic stress. The Mohr-Coulomb and Drucker-Prager yield descriptions, take into account the influence of hydrostatic stress and strain and can more realistically model non-linear behaviour of soils. With the Tresca and Mohr-Coulomb criterion it is assumed that yielding is independent of the intermediate normal stress.

Details of these yield criteria applicable to generalized two and three dimensional viscoplastic formulations can be found in References [1,20,28]. The von

Mises [29] and Mohr-Coulomb [26,27] yield functions have been used in the numerical stability analyses reported in this thesis since they have been used extensively in past engineering practice.

### 2.2.3 Simplifications for Two-Dimensional Problems

Since analyses of the problems given in this thesis are of a two dimensional nature, with  $\sigma = \langle \sigma_{11}, \sigma_{22}, \sigma_{33}, \sigma_{12} \rangle^T$  and  $\epsilon = \langle \epsilon_{11}, \epsilon_{22}, \epsilon_{33}, \gamma_{12} \rangle^T$ , any out-of-plane shearing action is zero, ie.,  $\sigma_{13} = \sigma_{23} = 0$ . The second stress invariant used in the von Mises description is then given by

$$J_2' = 1/2 [ (s_{11})^2 + (s_{22})^2 + (s_{33})^2 ] + (s_{12})^2 \quad (2.13)$$

Two dimensional plane strain conditions imply that one of the principal stress directions is out of plane and that the total out-of-plane normal strain  $\epsilon_{33}$  is zero. Assuming that the out-of-plane principal stress does not influence yielding and flow, the Mohr-Coulomb yield criterion for a two dimensional state of stress may be written as follows (see, Figure 2.4)

$$F = q + p \sin\phi - 2c \cos\phi = 0 \quad (2.14)$$

$$Q = q + p \sin\psi + \text{constant} \quad (2.15)$$

where  $q = [(\sigma_{11} - \sigma_{22})^2 + 4(\sigma_{12})^2]^{1/2}$  and  $p = (\sigma_{11} + \sigma_{22})$ . It should be noted that the definition of  $p$  and  $q$  used in this thesis is a factor of two larger than that traditionally used by others. The corresponding Tresca criterion can be easily derived for the case of  $\phi = \psi = 0$ .

Examples in this thesis are based on the two dimensional von-Mises yield criterion given by equation (2.9) and the Mohr-Coulomb descriptions given by equations (2.14) and (2.15). As was noted previously, the Mohr-Coulomb description is able to account for the influence of hydrostatic stress on the non-linear behaviour of the material of interest, whereas, the von-Mises criterion assumes yielding is independent of hydrostatic stresses. The intent of this thesis is to examine the numerical stability of transient behaviour. Although the reasons for selecting the Mohr-Coulomb and von-Mises yield descriptions are not based on the desire to model a particular material type, the simulations reported in this thesis use parameters acceptable for modelling geological materials such as soil and ice.

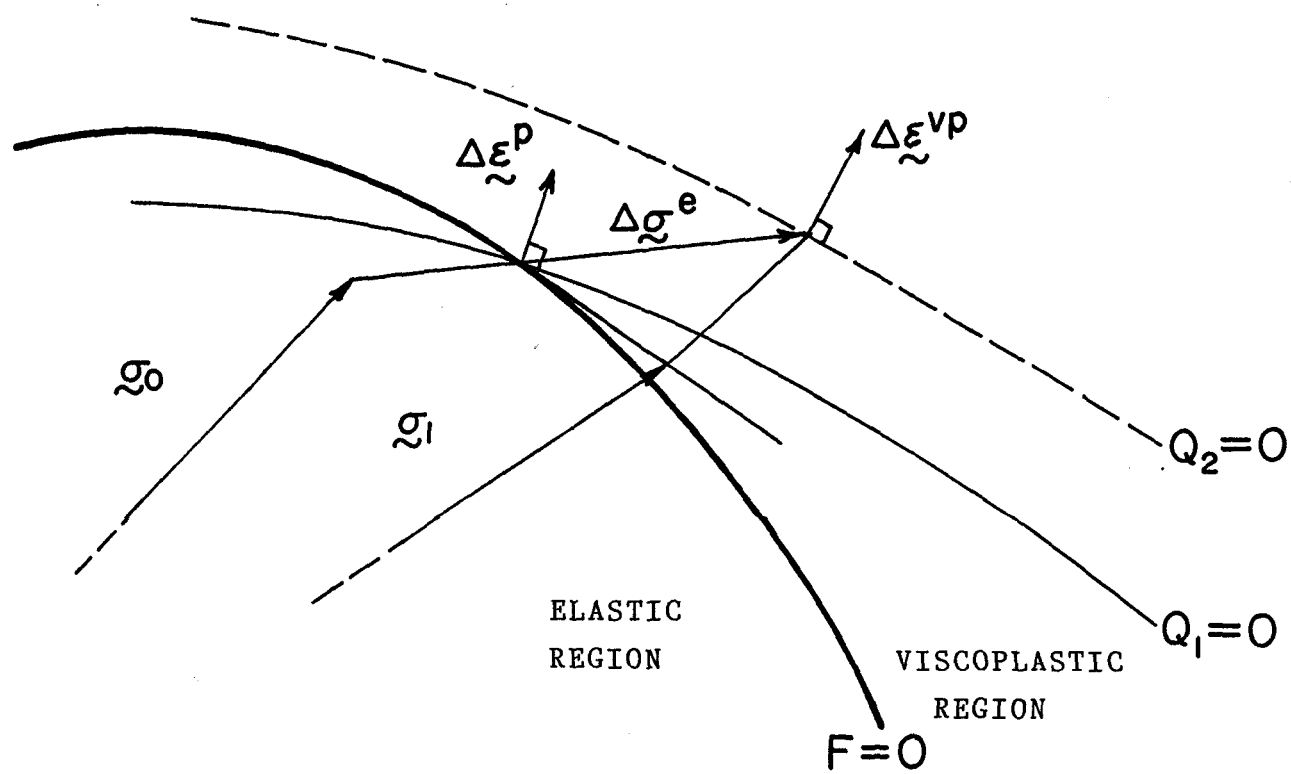


Figure 2.1 Elastic-Plastic/Viscoplastic Response

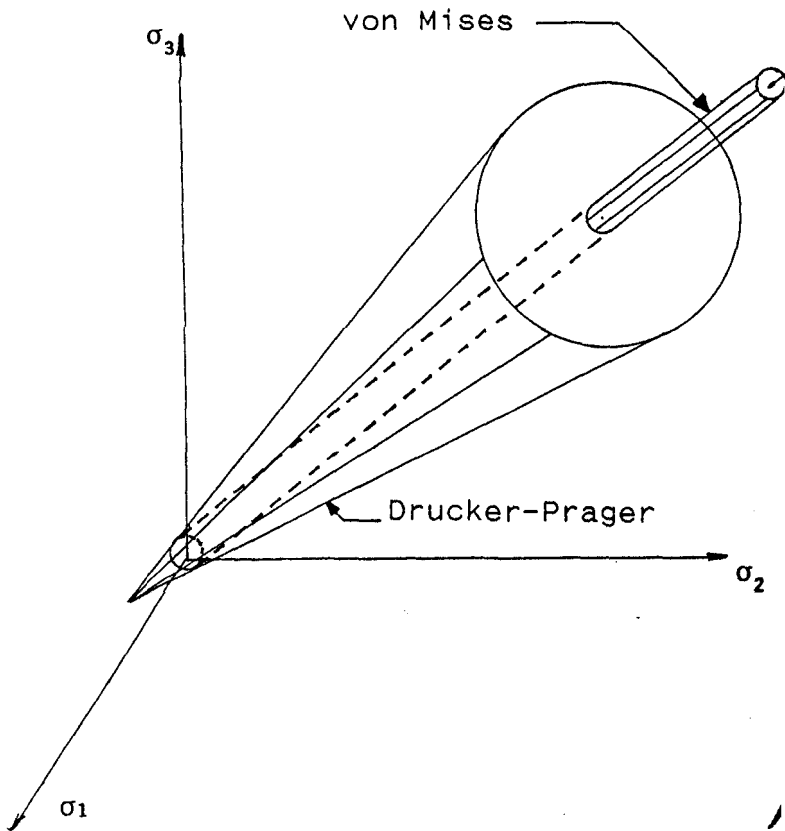


Figure 2.2 Drucker-Prager and von Mises Yield Description

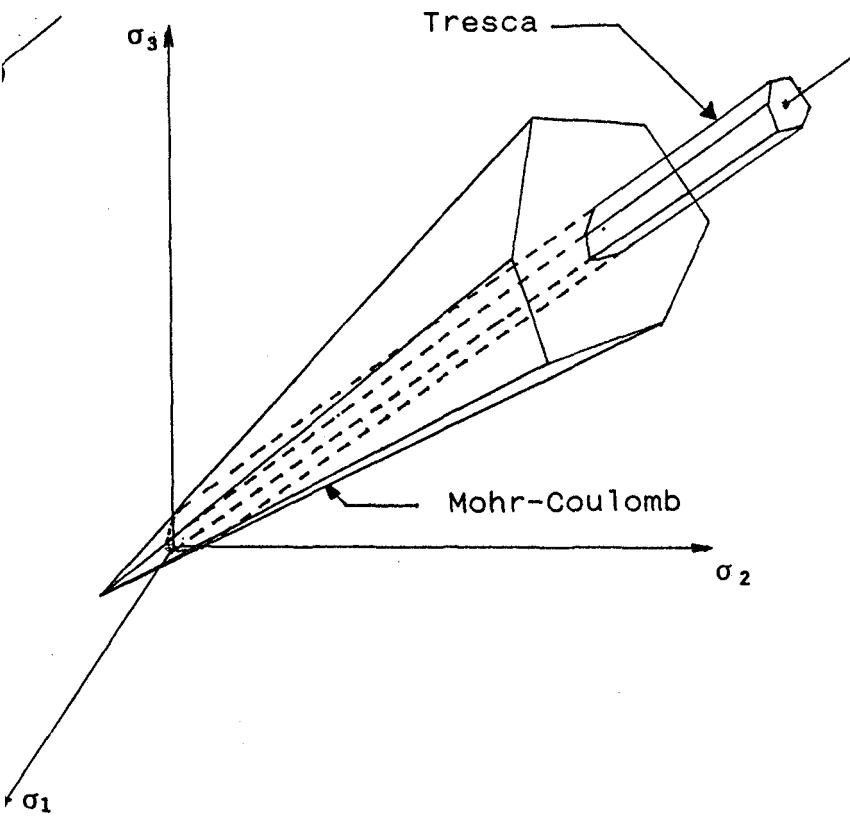


Figure 2.3 Mohr-Coulomb and Tresca Yield Description

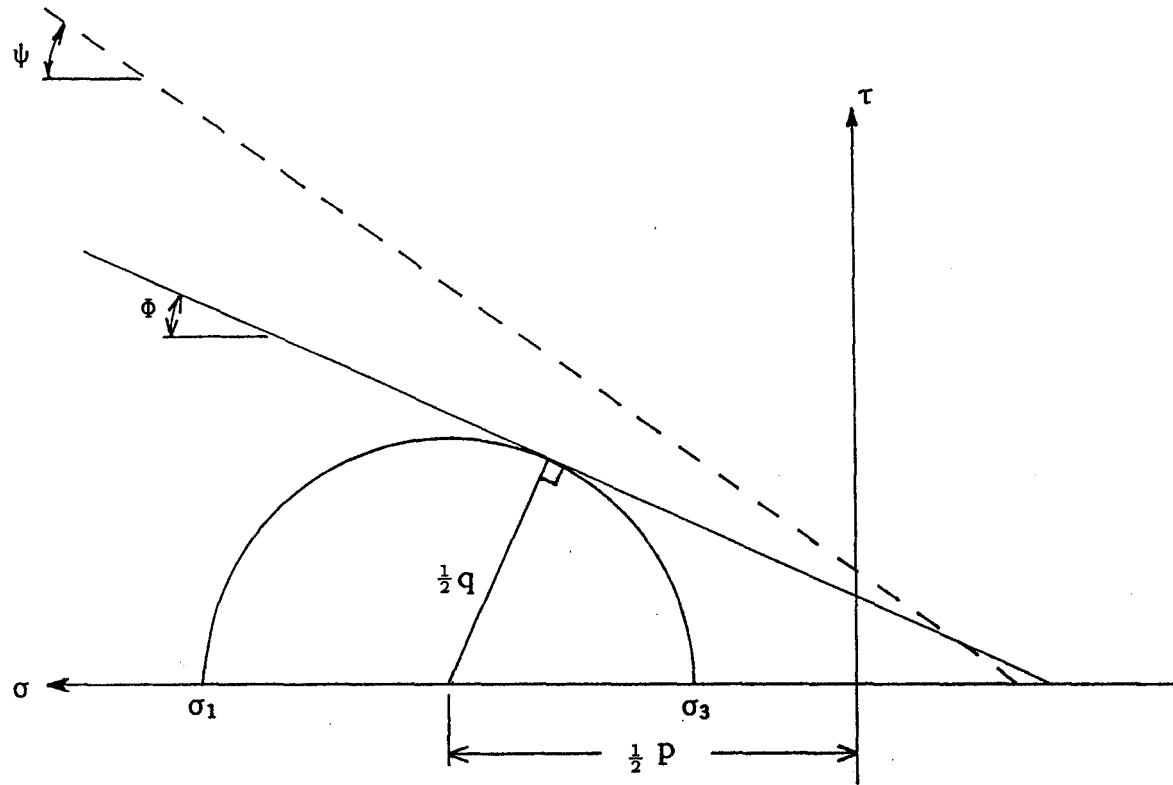


Figure 2.4 Mohr-Coulomb Two-Dimensional Yield Description

## CHAPTER 3

### NON-LINEAR FINITE ELEMENT FORMULATION

#### 3.1 General Non-Linear Finite Element Formulation

The finite element model which has been used in this study is formulated via a statement of virtual work. This section briefly outlines this procedure applicable to problems with small displacements, rotations and infinitesimal strains.

By considering the equilibrium of a body at some time,  $t_n$ , the total virtual work associated with this body due to an arbitrary virtual displacement,  $\delta u$ , is zero and can be expressed, after applying the divergence theorem, as follows:

$$\int_V \delta \epsilon_n^T \sigma_n dV - \int_V \delta u_n^T b_n dV - \int_S \delta u_n^T T_n dS = 0 \quad (3.1)$$

where  $\sigma_n$ ,  $\epsilon_n$  and  $u_n$  are vectors which contain the stresses, strains and displacements at any time  $t_n$ , respectively. The vectors  $b_n$  and  $T_n$  contain the internal body forces and boundary tractions, respectively.

Using the notion  $\epsilon_n = B u_n$  and  $u_n = N a_n$  [20] allows one to write the finite element equilibrium equation as

$$\Psi_n = \int_V B^T \sigma_n dV - R_n = 0 \quad (3.2)$$

where  $R_n = \int_V N^T b_n dV + \int_S N^T T_n dS$ , with  $B$  being the kinematic matrix relating total strains to displacements and  $N$  the matrix containing elemental shape functions which combine with the nodal degrees of freedom  $a_n$  to define the displacement field.

For non-linear problems, it is convenient to write Equation (3.2) in an incremental form. To achieve a suitable incremental form, consider equilibrium at the end of an increment of time,  $\Delta t_n = t_{n+1} - t_n$ . The corresponding stresses and applied loads at  $t_{n+1}$  are given as  $\Delta \sigma_{n+1} = \sigma_n + \Delta \sigma_n$  and  $R_{n+1} = R_n + \Delta R_n$ , respectively. Using these relations, Equation (3.2), corresponding to time  $t_{n+1}$ , can be expressed as

$$\Psi_{n+1} = \Psi_n + \int_V B^T \Delta \sigma_n dV - \Delta R_n = 0 \quad (3.2a)$$

A further modification of Equation 3.2 can be introduced by using an incremental form of a generalized Hooke's law,  $\Delta \sigma_n = D(\Delta \epsilon_n - \Delta \epsilon_n^{vp})$ , where  $\Delta \epsilon_n$  and  $\Delta \epsilon_n^{vp}$  represents the increment of total and irrecoverable viscoplastic strain at time  $t_n$ , respectively. The material matrix,  $D$ , is given in Reference [20] for various material types and geometric configurations. The material matrix applicable to isotropic material behaviour for axisymmetric and plane strain problems has been used in this thesis and is contained in Appendix B and C, respectively. After substituting a generalized Hooke's law into Equation (3.2a), the equation for equilibrium becomes

$$\Psi_{n+1} = \int_V \mathbf{B}^T \sigma_n dV + \int_V \mathbf{B}^T D(\mathbf{B} \Delta \mathbf{a}_n - \Delta \epsilon_n^{VP}) dV - R_{n+1} = 0 \quad (3.3)$$

Equation (3.3) yields the equilibrium equation which is used in the initial strain finite element method for viscoplastic analysis [1,20,28].

### 3.2 Elastic-Viscoplastic Implementation for Plasticity

If a stress measure  $\sigma_n^\dagger$  is introduced such that  $\sigma_n^\dagger = \sigma_n - D \Delta \epsilon_n^{VP}$ , Equation (3.3) reduces to the following form

$$\Psi_{n+1} = \int_V \mathbf{B}^T \sigma_n^\dagger dV + \int_V \mathbf{B}^T D \mathbf{B} dV \Delta \mathbf{a}_n - R_{n+1} = 0 \quad (3.4)$$

Equation (3.4) has the appearance of the equilibrium equation that is used for initial stress analysis of plasticity problems [30]. The calculation of  $\sigma_n^\dagger$  represents a stress level in which a stress updating is carried out at the beginning of a time step rather than at the end which is typical of initial strain algorithms. The point that is being made here is that both the initial strain and stress methods, although conceptually different [28,31], are numerically the same for plasticity problems since they involve the same algorithm; only the book-keeping of stresses is different. For the initial stress approach, the stress level  $\sigma$  is represented by  $\sigma_n^\dagger$  rather than by  $\sigma_n$ . Since both the initial

stress and strain methods are numerically the same, one would expect similar solutions for a particular boundary-valued problem from both. It is most likely that the small differences which have been reported in the literature, are due to the details concerning the treatment of  $\Delta \epsilon^p$  and not because of the differences between the solution techniques.

Although various iterative time marching schemes for the solution to viscoplasticity problems have been reported in literature, the initial strain method, using an explicit time-marching scheme, still appears to be preferred. This is because it is simple to implement into finite element programs and provides sufficient accuracy with reasonable computational effort [28]. In particular, researchers have shown that the implicit scheme, which requires inversion of the stiffness matrix during each iteration, may require considerable computational effort. This occurs especially in cases of non-associated viscoplasticity where the stiffness matrix is non-symmetric [31,32]. The explicit scheme avoids this problem since the stiffness matrix is constant and only needs to be inverted at the beginning of a simulation or load increment [1,31]. One requirement of an explicit approach is that the choice of the time step size must be small enough to ensure solutions are numerically stable and accurate [15]. The next chapter will address the topic of numerical stability for modelling viscoplasticity using an explicit approach.

### 3.3 Overview

The results of simulations which are reported in the following chapters have been obtained by using the explicit initial strain approach. This iterative approach is also used together with load incrementing [6,10,20] for solving plasticity problems. The load increment method has been chosen in order to speed up the rate of convergence of the iterative solutions as suggested by several researchers [1,20] and to obtain a trace of the stress-strain and load-deflection histories at various points.

## CHAPTER 4

### NUMERICAL STABILITY IN VISCOPLASTICITY

#### 4.1 General

The major distinctions between the explicit and implicit time-stepping techniques are well documented [1]. In general, as mentioned in Chapter 3, explicit time-marching strategies for nonlinear viscoplasticity require sufficiently small time steps to maintain numerical stability; therefore more iterations are required for convergence. The implicit algorithm remains stable with larger time steps; thus convergence is reached with fewer iterations. Unfortunately, implicit methods demand considerably more computational effort for each time step when compared with explicit methods, since the stiffness matrix must be inverted for each step. In the past, both methods have received considerable attention for solving problems in viscoplasticity. The computational effectiveness of an explicit method is related to the ability of obtaining a good estimate for the maximum permissible time step size,  $\Delta t$  [15]; that is, the largest time step for which a numerically stable solution can be obtained. The purpose of this chapter is to demonstrate a simple, yet effective, technique which can be used to obtain a general stability

criterion for explicit time stepping schemes involving the initial strain method for viscoplasticity.

#### 4.2 Literature Review on Viscoplastic Numerical Stability

The most significant treatment of numerical stability of explicit time-marching for viscoplasticity was given by Cormeau [15] in 1975. Unfortunately, in his mathematically eloquent treatment of numerical stability, he had to restrict his analysis to non-hardening and associated viscoplasticity in order to make use of well known properties of matrices and their eigenvalues. Also owing to the nature of his analysis, explicit criteria could only be obtained for simpler viscoplastic flow rules. This contribution was significant since previous stability criteria were based solely on conservative empirical relations [1].

An extension to the work of Cormeau on stability was given by Owen and Damjanic [8]. In their work, they investigated both explicit and conditionally stable implicit schemes. For the explicit approach, they obtained a criterion that was less conservative than that developed by Cormeau [15]; i.e., Cormeau's approach yields criteria that are very conservative for problems that are nearly statically determinate or kinematically unconstrained [8]. As with Cormeau's stability criterion, Owen and Damjanic's proposed

criterion was restricted to an associative flow law.

More recently, Nicholson [16] addressed the problem of stability for non-associative viscoplasticity. Nicholson was able to overcome the difficulties associated with the resulting non-symmetric matrices used in non-associated viscoplasticity. In particular, he used general eigenvalue bounds on the non-symmetric matrices of the non-associated model to obtain a criterion for stability.

Telles and Brebbia [7], by considering the case of pure stress relaxation, developed a stability criterion which could also take into account hardening and softening behaviour. Their approach which is similar in nature although less general to that proposed in this study, yielded a maximum time step identical to that obtained by Cormeau [15] for creep problems based on a von Mises criterion and with  $\nu \rightarrow 0.5$ .

Most recently, Benallal [13,17] used an approach similar to that of Cormeau to obtain a stability criterion which also accounts for isotropic and kinematic hardening and softening. His stability criterion is identical to that of Cormeau [15] for the explicit case and that of Hughes and Taylor [18] for the semi-implicit case. Benallal [17] obtained an expression for maximum time step which is identical to that of Telles and Brebbia [7] for a hardening von Mises material.

In the following Sections an intuitive approach is

presented to obtain general numerical stability criteria, for explicit time marching schemes. The resulting criteria are applicable for material descriptions incorporating associative or non-associated, and hardening viscoplasticity. The value of the approach rests in its simplicity and in its interpretation.

#### 4.3 Numerical Stability for One Dimensional Problems

In order to demonstrate problems associated with numerical stability, a simple uniaxial stress problem is analyzed first. Two cases are considered as follows: (1) constant stress creep; and (2) constant strain creep (creep relaxation) [8].

Consider first a bar of uniform cross section subjected to a constant load  $P$  as shown in Figure 4.1. For such problems the stress rates are related to strain rates via the constitutive equation  $\dot{\sigma} = E (\dot{\epsilon} - \dot{\epsilon}^c)$ . In this case,  $\dot{\sigma} = 0$ , and thus  $\dot{\epsilon} = \dot{\epsilon}^c$ . By utilizing the well known power law for creep the following relationship is obtained

$$\dot{\epsilon} = \dot{\epsilon}^c = A |\sigma|^{n-1} \sigma \quad (4.1)$$

An approximate solution to Equation (4.1) can be obtained by using Euler's explicit time stepping scheme as follows:

$$\varepsilon_{n+1} = \varepsilon_n + A |\sigma_n|^{m-1} \sigma_n \Delta t_n \quad (4.2)$$

It may be noted that stability is maintained for all  $\Delta t_n$ , only the accuracy of the solution changes.

Let us now consider the second case, in which the bar is deformed instantaneously and is then held such that the subsequent total strain increment is zero, as shown in Figure 4.2. At the moment of loading, the response is fully elastic, thereby yielding an initial uniaxial stress  $\sigma_0 = E\varepsilon$ . Since  $\varepsilon = 0$ , the equation governing changes in stress with time is given as

$$\dot{\sigma} = -EA |\sigma|^{m-1} \sigma \quad (4.3)$$

This equation reduces to the form

$$\dot{\sigma} + \mu |\sigma|^{m-1} \sigma = 0 \quad (4.4)$$

with  $\mu = -EA$ . The following closed form solutions exist

$$\sigma = \sigma_0 e^{-\mu t} \quad \text{for } |m| = 1 \quad (4.5)$$

$$\sigma = [ (m-1)\mu t + \sigma_0^{(1-m)} ]^{1/(1-m)} \quad \text{for } |m| \neq 1 \quad (4.6)$$

By examining these solutions, it is clear that the transient response is of a decay nature.

Using a finite difference equivalent of Equation (4.4) with an Euler time-marching scheme, the solution for this equation can be expressed in an approximate form by the following recursion equation

$$\sigma_{n+1} = \sigma_n (1 - \mu \Delta t_n |\sigma_n|^{n-1}) \quad (4.7)$$

The numerical solution to such a recursion equation can only remain stable for  $\Delta t_n$  less than some upper bound on time step. Based on comparing the numerical and closed form solutions of Equation (4.4), it is possible to identify three levels of stability:

$$\Delta t < \Delta t_{\max} = (1/\mu |\sigma_n|^{n-1}) \quad \text{:stable no oscillations:} \quad (4.8)$$

stress decreasing

asymptotically

$$\Delta t_{\max} < \Delta t < 2 \Delta t_{\max} \quad \text{:stable with oscillations:} \quad (4.9)$$

stress oscillates with

decreasing amplitude

$$\Delta t > \Delta t_{\text{crit}} = 2 \Delta t_{\max} \quad \text{:unstable:} \quad (4.10)$$

stress oscillates with

increasing amplitude

Figures 4.3 and 4.4 show the transient responses related to Equation (4.7) for a linear case ( $m=1$ ) and nonlinear case ( $m=3$ ), respectively. If the maximum time step

size,  $\Delta t_{\max}$ , is not exceeded the numerical time stepping solution converges while remaining stable with no oscillations. Using a time step size between  $\Delta t_{\max}$  and  $\Delta t_{\text{crit}}$  the numerical solution converges with stable oscillations. If a critical time step  $\Delta t_{\text{crit}}$ , is exceeded then solutions become unstable and do not converge.

In the previous section, the case of pure stress relaxation was used to obtain a stability criterion for a uniaxial creep problem. By investigating the stress relaxation characteristics at the highly stressed points of any boundary-value problem in a similar manner, it should be possible to obtain a stability criterion for a more general multi-dimensional problem with a more complex yield criterion and material behaviour. This is the philosophy adopted in this thesis. Before introducing the approach proposed in this thesis, the traditional eigenvalue approach used for multidimensional problems for obtaining a stability criterion is briefly discussed in the following section. The brief review is given in order to help demonstrate the difference between the approach described herein and traditional ones.

#### 4.4 Traditional Approach for Numerical Stability

The numerical stability of explicit time-marching schemes for non-linear, first order systems of differential equations applicable to elastic-viscoplasticity was

investigated by Cormeau [15] in 1975. The first step in his analysis was to convert Equation 3.3 into a system of nonlinear differential equations

$$d\Sigma/dt = f(\Sigma) \quad (4.11)$$

where  $f$  represents a system of nonlinear functions of  $\Sigma$  which is a vector containing stresses at all numerical integration points. Through a piece-wise linearization of  $f$  using a truncated Taylor's expansion, Equation (4.11) takes on the linear form

$$d\Sigma/dt = f(\Sigma_n) + J_n (\Sigma - \Sigma_n) \quad (4.12a)$$

$$d\Sigma/dt = J \Sigma + C \quad (4.12b)$$

where  $C = f(\Sigma_n) - J_n \Sigma_n$  represents a constant and  $J = \partial f / \partial \Sigma$ , which depends on the viscoplastic description, is the Jacobian matrix of  $f$ .

Cormeau [15] suggested that Equation (4.11) remains stable provided that the time intervals are kept within the limits

$$0 < \Delta t_n < 2 / \lambda_{\max} \quad (4.13)$$

where  $\lambda_{\max}$  is the largest eigenvalue of the Jacobian matrix

J. Since a full eigenvalue analysis of  $J$  is a lengthy process itself, simplifications were introduced via Rayleigh's Quotient. Where possible, a further simplification was made, by obtaining analytical forms of  $\lambda_{\max}$ . This was done to avoid the lengthy computation time associated with computing  $\lambda_{\max}$  at every integration point. The point which the author wishes to elude to in this section is that closed form stability criteria for complex material descriptions are not easily obtained via an eigenvalue analysis.

#### 4.4 Proposed Approach for a Numerical Stability Criterion

In order to understand the proposed approach, it is essential to focus on the physical response of a body which is undergoing viscoplastic deformation. During the time-dependent deformation there is a redistribution of stresses in the body such that the yield function  $F$ , and hence the flow function  $\langle \phi(F) \rangle$ , decreases with time at every point in the body where  $F > 0$ . This suggests that the numerical stability may be analyzed by studying how  $\Gamma = A \langle \phi(F) \rangle$  decays with time in the region where the body is stressed the greatest. To do this,  $\Gamma$  is expanded by using a truncated Taylor's expansion:

$$\Gamma_{n+1} = \Gamma_n + \Gamma' [(\partial F / \partial \sigma_n)^T \Delta \sigma_n + (\partial F / \partial \kappa_n) \Delta \kappa_n] \quad (4.14)$$

where  $\partial F / \partial \sigma_n = \langle \partial F / \partial \sigma_{11}, \partial F / \partial \sigma_{22}, \partial F / \partial \sigma_{12}, \partial F / \partial \sigma_{33} \rangle^T$ ,  
 $\Gamma' = \partial \Gamma / \partial F$  and  $\kappa$  represents a hardening parameter such as volumetric or deviatoric plastic strains. The other terms are the same as defined previously. Substituting the non-associative flow rule, ie. Equation (2.1), and a Generalized Hooke's law into (4.14), and using an explicit time-marching scheme yields:

$$\Gamma_{n+1} = [ 1 - \Gamma' ( H_e + H_p ) \Delta t_n ] \Gamma_n + ( \partial F / \partial \sigma_n )^T D \Delta \epsilon_n \quad (4.15)$$

where  $H_e = (\partial F / \partial \sigma_n)^T D (\partial Q / \partial \sigma_n)$ ,  $H_p = -(\partial F / \partial \kappa) (\partial \kappa / \partial \epsilon_n)^T (\partial Q / \partial \sigma_n)$  is a viscoplastic hardening parameter and  $\partial Q / \partial \sigma = \langle \partial Q / \partial \sigma_{11}, \partial Q / \partial \sigma_{22}, \partial Q / \partial \sigma_{12}, \partial Q / \partial \sigma_{33} \rangle^T$ . By analyzing the worst case which is pure stress relaxation [7,8,15], ie.,  $\Delta \epsilon_n = 0$ , and noting the similarities between Equations (4.15) and (4.7), the numerical stability criterion can be directly written as:

$$\Delta t \leq \Delta t_{\max} = \frac{1}{\Gamma' (H_e + H_p)} \quad (4.16)$$

for the case where oscillations are not allowed. By considering pure relaxation as the worst case for numerical stability, Equation (4.16) gives an estimate for the maximum time step. At this point it should be noted that if oscillatory stability behaviour is acceptable, a second bound given by  $\Delta t_{\text{crit}} = 2 \Delta t_{\max}$  can be used as a stability criterion. While overall non-oscillatory behaviour of  $\Gamma$  is maintained for

$\Delta t < \Delta t_{\max}$ , it may be possible that certain individual stress components may oscillate, since the stability criterion is based on examining the behaviour of the scalar function  $\Gamma$ .

For a hardening material where  $H_p > 0$ ,  $\Delta t_{\max}$  is overestimated when ignoring the influence on the maximum time step. This was also observed by Telles and Brebbia [7] for the case of a von Mises yield criterion.

In the application of Equation (4.16) an important assumption is made; ie., it is assumed that non-oscillatory stability of the overall problem can be maintained, provided that oscillations can be suppressed at the most critical point in the domain [8]. The validity of this assumption for associated viscoplasticity has been shown in a formal manner by Cormeau [15]. As will be shown in examples presented in the following sections, this assumption may, for some problems, provide an extremely conservative estimate of critical time step.

Equation (4.16) has been applied to Mohr-Coulomb and von Mises yield functions which are used to solve problems that are presented in the following chapters. The numerical stability criteria based on these yield functions are given in the next section for cases of non-hardening.

One last point should be made before leaving this section. That is, Equation (4.14) can be used to derive an implicit elastic-viscoplastic constitutive matrix. In order to avoid taking the emphasis away from stability, a brief

derivation of the implicit scheme is given in Appendix A. The advantage of using a fully implicit scheme results from the fact that unconditional stability is guaranteed and only the desired accuracy limits the time step size used [8].

#### 4.5 Examples of Numerical Stability Criterion Expressions

The application of Equation (4.16) to a non-associative constitutive description using the plane strain Mohr-Coulomb yield criterion given in Chapter 2, results in the following criterion for non-oscillatory stability:

$$\Delta t_{\max} = \frac{(1+\nu)(1-2\nu)}{2m F^{n-1} EA(1-2\nu+\sin\phi \sin\psi)} \quad (4.17)$$

where  $E$  is the elastic modulus,  $\nu$  is Poisson's ratio and the other terms are the same as described previously. It can be shown for associated viscoplasticity, that  $\Delta t_{\max} = \Delta t_{\text{crit}} / 2$  is exactly the same as that given by Cormeau [15]. It is clear from Equation (4.17) that the stability of a viscoplastic time marching scheme is sensitive to both  $\phi$  and  $\psi$ .

For the Tresca case of  $\phi = \psi = 0$ , the following stability criterion is obtained

$$\Delta t_{\max} = \frac{(1+\nu)}{2EAmF^{n-1}} \quad (4.18)$$

For a von Mises material the stability criterion is given by

$$\Delta t_{\max} = \frac{2(1+\nu)}{3E\Delta m F^{n-1}} \quad (4.19)$$

Detailed derivations of the aforementioned maximum time steps are contained in Appendix C. The applicability of these criteria are examined in the next chapter. Maximum time steps for the volumetric and the deviatoric material descriptions are presented in Appendix B. The author is not familiar with any literature that provides a numerical stability criterion for the latter two material descriptions.

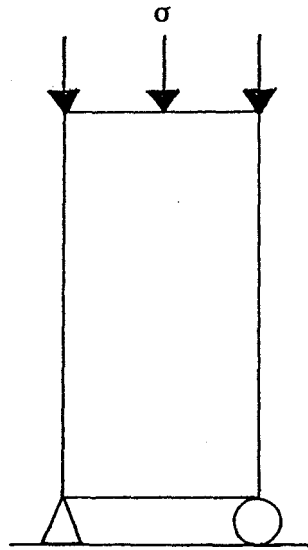


Figure 4.1 One-Dimensional Constant Stress  
Creep Configuration

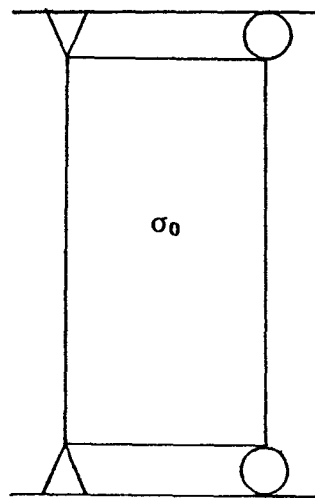


Figure 4.2 One-Dimensional Constant Strain  
Creep Configuration

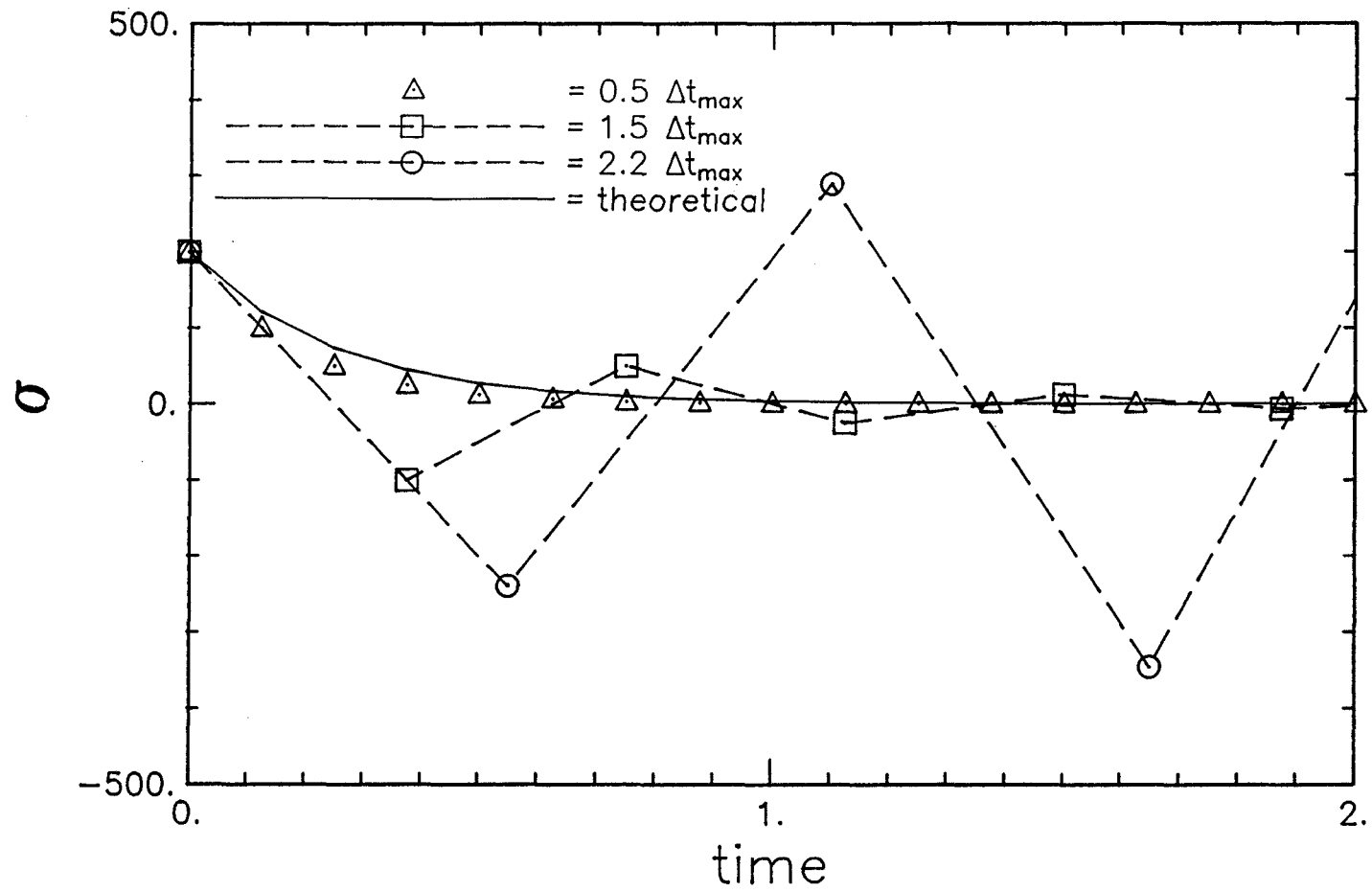


Figure 4.3 One-Dimensional Instability Demonstration :  $m = 1$

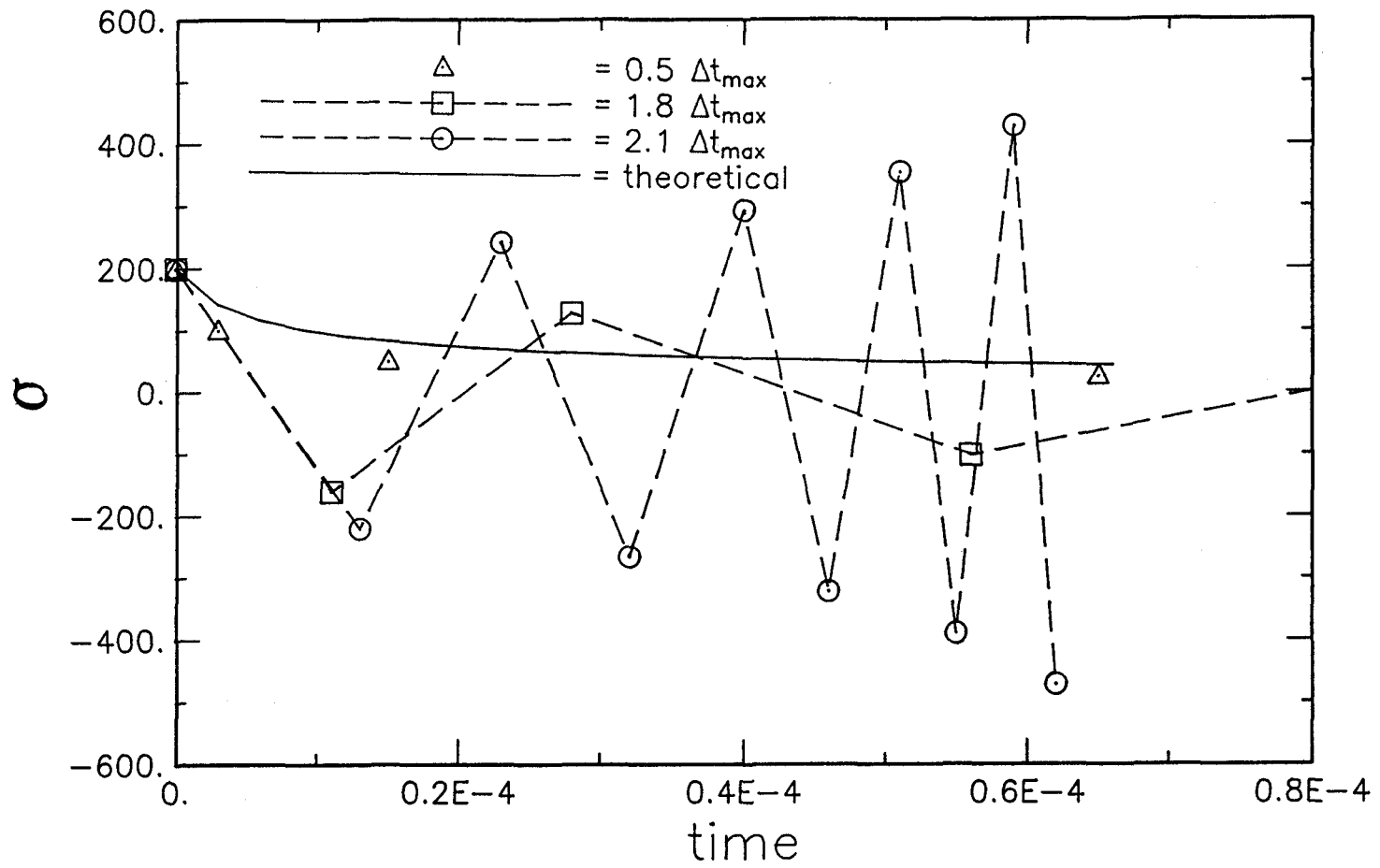


Figure 4.4 One-Dimensional Instability Demonstration :  $m = 3$

## CHAPTER 5

### ELASTIC AND VISCOPLASTIC FINITE ELEMENT SIMULATIONS

#### 5.1 Introduction

This chapter contains examples of specific boundary-valued problems which were modelled using a non-linear, time-dependent finite element model. The finite element program which was modified for this study, was verified by comparing finite element and closed-form solutions for both linear elastic and creep boundary-value problems. The first example demonstrates that the finite element model is capable of simulating elastic results for a strip loaded footing. The second example was used to compare elastic and creep solutions for a thick-walled cylinder. For all simulations, the eight-noded isoparametric element was used.

#### 5.2 Comparison with Steady State Creep and Elasticity

In the first example, which was used to verify the finite element program, the author modelled a flexible strip footing on an elastic half space as shown in Figure 5.1. The elastic modulus,  $E$ , and Poisson's ratio,  $\nu$ , used for the simulations were 4800 kPa and 0.2, respectively [33]. The

theoretical results for normal and shear stresses, are given in Reference [34].

Figures 5.2, 5.3 and 5.4 compare the theoretical and finite element solutions for normal and shear stress variations with depth, respectively. These results, are given for horizontal locations, corresponding to integration points at,  $x = 0.106m \approx 0.0$  and  $x = 1.12m \approx a$ ; where the footing width 'a' was equal to 1.0 metres. As shown, the finite element results compare well with theory. The small differences in the results are attributed to the finite element discretization and to the fact that the theory assumes a semi-infinite half-space whereas the finite element model contains boundaries which are finite distances away.

The second example is that of an axisymmetric thick-walled cylinder, shown in Figure 5.5, which is loaded with a uniform pressure on the inside face and which is allowed to creep until steady state conditions are achieved. For this problem, the prediction of radial stress variation through the thickness of the cylinder for both elastic and steady state creep was obtained. The closed form solution for a von Mises material can be found in reference [35] on creep analysis and is given as follows:

$$\sigma_r = -p_i \frac{(r^{-2/n} - r_0^{-2/n})}{(r_i^{-2/n} - r_0^{-2/n})} \quad (5.1)$$

in which  $m$  is a power law exponent;  $r_i$  and  $r_0$  are the inner and outer radii of the cylinder, respectively;  $r$  is the radial distance where the stresses of interest are determined; and  $p_i$  is the applied pressure. It should be noted that Equation (5.1) is independent of  $A\langle\phi(F)\rangle$ , and the elastic properties  $E$  and  $\nu$ . More details of the creep law are given in the following section.

Figure 5.6 shows, both, the predicted elastic and steady state creep radial stress variations with those obtained from the closed form solutions. The steady state creep results are given for a linear ( $m=1$ ) and non-linear ( $m=3$ ) creep power law. The elastic solution can be obtained from Equation (5.1) by letting  $m = 1$ ; see eg. Reference [35]. As in the first example the finite element solutions compare exceptionally well to closed-form solutions, thereby suggesting that the finite element model used for this study was free of major computer coding errors when applied to elastic and creep simulations.

### 5.3 Numerical Instability Associated with Creep Problems

The emphasis in the previous two problems was on verifying the finite element algorithm; the next few examples address numerical stability applied to creep problems. The standard power law creep problem is modelled where the yield

stress is reduced to zero. The result is that finite creep strain rates exist at all levels of stress.

### 5.3.1 Stress Relaxation Problems

In the first example of this section, the results of pure stress relaxation for an axisymmetric stress configuration are presented. In this problem, as shown in Figure 5.7, all edges of the boundary were constrained; ie.,  $\Delta\epsilon_{11} = \Delta\epsilon_{22} = \Delta\epsilon_{33} = 0$ . Initial stresses were introduced via initial strains, as described in Reference [5]. Although this problem could have been easily solved using a hand calculator, the finite element method was used. This analysis provided a further check on the finite element code.

The following multi-axial creep law using a von Mises yield criterion was incorporated into a finite element program

$$\dot{\epsilon}_{ij}^{VP} = 3/2 A \sigma_e^{m-1} s_{ij} \quad (5.2)$$

where  $\sigma_e = (3J_2')^{1/2}$ ;  $A=10^{-4} \text{ yr}^{-1} \text{ kPa}^{-1}$  for a linear creep law ( $m=1$ ) and  $A=10^{-8} \text{ yr}^{-1} \text{ kPa}^{-3}$  for a non-linear creep law ( $m=3$ ). These were found to be acceptable constants for modelling geological materials susceptible to creep [36]. An elastic modulus of 907500 kPa and Poisson's ratio of .34 were the elastic material properties used.

Since creep is a function of only  $J_2'$ , it was

necessary in this example to apply initial strains which produced an initial non-hydrostatic stress state. These initial strains are given as follows:

$$\varepsilon_{11}_0 = \varepsilon_{22}_0 = .001, \varepsilon_{33}_0 = .0005, \varepsilon_{12}_0 = 0 \quad (5.3)$$

The maximum permissible time step, according to Equations (4.19) and (5.2) is given by,

$$\Delta t_{\max} = \frac{2(1+\nu)}{3E\alpha_m \sigma_e^{m-1}} \quad (5.4)$$

This stability criterion is consistent with the one developed by Cormeau [15] where  $\Delta t_{\text{crit}} = 2 \Delta t_{\max}$  for a material obeying a von Mises criterion.

Figure 5.8 shows that for the linear creep law, the numerical stability criterion is satisfied exactly. For the case of a non-linear creep law (ie.,  $m = 3$ ), the numerical stability criterion was not able to predict the limiting stability of the system accurately, as shown in Figure 5.9. The criterion given by Equation (5.4) however, did provide a conservative estimate of the maximum time step for a non-linear creep law.

Since the numerical stability criterion was unable to accurately predict the limiting stability for the case of a non-linear creep law, a second possible stability criterion

was studied where changes in the yield function  $F$ , rather than in  $\Gamma$ , were considered. Following the same procedure used for obtaining a stability criterion based on changes in  $\Gamma$ , the following stability criterion can be developed for  $F$

$$\Delta t_{\max}^F = \frac{F}{\Gamma(H_e + H_p)} \quad (5.5)$$

which for a von Mises material description, with  $H_p=0$ , can be written as follows:

$$\Delta t_{\max}^F = \frac{2(1+\nu)}{3EA \sigma_e^{n-1}} = m \Delta t_{\max} \quad (5.6)$$

As shown above, the criterion for  $\Delta t_{\max}^F$  is equal to  $\Delta t_{\max}$  times the power law creep exponent  $m$ . Figures 5.8 and 5.9 demonstrate that this alternative criterion was able to provide a better estimate of the actual  $\Delta t_{\text{crit}}$  ( $= 2 \Delta t_{\max}$ ) than the previous criterion based on  $\Gamma$ . Recall that  $\Delta t_{\text{crit}}$  represents a limit on oscillatory stability whereas  $\Delta t_{\max}$  represents a limit on non-oscillatory stability.

The next example presented in this section, is similar to the previous one except that the radial boundary was free to move and the initially applied strains were as follows:  $\epsilon_{11_0} = \epsilon_{22_0} = \epsilon_{33_0} = .001$  and  $\epsilon_{12_0} = 0$ . The results shown in Figures 5.10 and 5.11, reveal that the

observed critical time step (  $\Delta t_{crit}$  ) is greater than that for the previous case where all sides were constrained.

Owing to the simple state of stress of this problem, it is possible to obtain a closed-form maximum time step by reducing the problem to one-dimensional form as given in Appendix D. The results of such an algebraic exercise reveal that the maximum time step yielding non-oscillatory behaviour is given by

$$\Delta t_{max}^{1D} = \frac{1}{AE \sigma_e^{m-1}} \quad (5.7)$$

Comparison of Equations (5.4) and (5.6) to (5.7), yields the following relationship:

$$\Delta t_{max}^{1D} = \frac{3m}{2(1+\nu)} \Delta t_{max} = \frac{3}{2(1+\nu)} \Delta t_{max}^F \quad (5.8)$$

It is clear from this equation, that for a nonlinear creep law, the stability criterion based on  $\Gamma$  is very conservative.

If one were to substitute into Equation (5.8) the appropriate material properties for this problem, the resulting non-oscillatory estimates on time step would be:

$$\Delta t_{max}^{1D} = 1.12 \Delta t_{max} , \quad \text{for } m = 1 \quad (5.9)$$

$$\Delta t_{max}^{1D} = 3.36 \Delta t_{max} , \quad \text{for } m = 3 \quad (5.10)$$

Figures 5.10 and 5.11 verify these calculations since non-oscillatory stability is preserved for  $1.1 \Delta t_{\max}$  for the linear ( $m=1$ ) case and for  $3.25 \Delta t_{\max}$  for a nonlinear ( $m=3$ ) creep law.

For the case of unstable oscillatory behaviour, the estimated critical time steps  $\Delta t_{\text{crit}}$  ( $= 2 \Delta t_{\max}$ ) are given by

$$\Delta t_{\text{crit}}^{1D} = 2.24 \Delta t_{\max} \quad , \quad \text{for } m = 1 \quad (5.11)$$

$$\Delta t_{\text{crit}}^{1D} = 6.72 \Delta t_{\max} \quad , \quad \text{for } m = 3 \quad (5.12)$$

As can be seen from Figures 5.10 and 5.11, the unstable behaviour was observed with  $\Delta t > 2.24 \Delta t_{\max}$  for linear creep ( $m=1$ ) and with  $\Delta t > 6.72 \Delta t_{\max}$  for nonlinear creep ( $m=3$ ).

The purpose of presenting this example was to compare the general numerical stability criterion of Equation (4.16) for a problem in which the actual  $\Delta t_{\max}$  can be easily calculated from equilibrium. Since the actual  $\Delta t_{\max}^{1D}$  takes into account the level of constraint and  $\Delta t_{\max}$  does not, the difference in results indicate that numerical stability is strongly dependant on the level of constraint as anticipated. In general, it may be said that as the degree of constraint leading to stress redistribution is reduced, the maximum permissible time step increases. Unfortunately, for general boundary-value problems, the level of constraint within the domain is not known, a priori.

Equation (5.8) also reveals that the stability

criterion based on  $F$  for nonlinear creep ( $m=3$ ) yields a much better estimate of a maximum time step than that based on  $\Gamma$  for this particular problem. While it is tempting to adopt this criterion for stability, the example presented in the following section demonstrates that for some problems this criterion may not be strict enough.

### 5.3.2 Creep of a Thick-Walled Cylinder - Instability

The thick-walled cylinder as shown in Figure 5.5 was modelled for creep using a von Mises yield criterion (see example in section 5.2). The material properties for the simulations presented in this section are the same as those used in the previous section.

Figure 5.12 and 5.13 show the axial stress, at the integration point nearest to the inside wall, verses time for linear ( $m=1$ ) and non-linear ( $m=3$ ) creep, respectively. The results are shown for time steps relative to the maximum time step based on the truncated Taylor's expansion of  $\Gamma$ .

The results of the simulations for the linear creep law ( $m=1$ ) shown in Figure 5.12 indicate that oscillations and instability occurred when the proposed stability criterion was not satisfied. Figure 5.13 shows that for cases of non-linear creep ( $m=3$ ) the stability criterion is conservative since the solution remained stable even for  $\Delta t > 2.5 \Delta t_{\max}$ . This leads one to consider using the criterion based on  $F$ . The

relationship between the stability criterion based on  $F$  and  $\Gamma$ , as indicated by Equation (5.6), can be expressed as

$\Delta t_{\text{max}}^F = 3 \Delta t_{\text{max}}$ . By basing stability on  $F$ , one would expect non-oscillatory stability for  $\Delta t < 3 \Delta t_{\text{max}}$ . As shown in Figure 5.13, the stresses oscillated for  $\Delta t < 3 \Delta t_{\text{max}}$ , which is contrary to  $\Delta t_{\text{max}}^F$ .

It is apparent from this example that a stability criterion for non-oscillatory behaviour based on  $F$  is not strict enough. If one were to use this less restrictive criterion, results may become unstable for certain problems, indicating an unacceptable shortcoming. The criterion based on  $\Gamma$  produced conservative predictions for all examples shown. In the remainder of this thesis only the stability criterion given by Equation (4.16) and a linear creep power law ( $m=1$ ) is considered.

#### 5.4 Elastic/viscoplastic Instability

The example presented in this section is used to demonstrate the stability behaviour of a elastic/viscoplastic material in which, contrary to creep problems, viscoplastic strain rates may cease for non-zero  $J_2'$ . A typical situation where this could arise is when a Mohr-Coulomb yield criterion is used with a non-zero frictional angle and/or cohesion.

The geometry of this problem is similar to that shown in Figure 5.7 except that the solution here is for a plane

strain condition with the horizontal direction boundary unconstrained. A Mohr-Coulomb criterion, corresponding to the following yield function, also given in Chapter 2, is expressed as follows:

$$F = q + p \sin\phi - 2c \cos\phi = 0 \quad (5.13)$$

where  $q = [(\sigma_{11} - \sigma_{22})^2 + 4(\sigma_{12})^2]^{1/2}$ ,  $p = (\sigma_{11} + \sigma_{22})$ ,  $\phi$  is the material friction angle and  $c$  is the cohesion. Initial strains were applied such that  $\varepsilon_{11}_0 = \varepsilon_{22}_0 = .005$  and  $\varepsilon_{12}_0 = 0$ . A friction angle of 30 degrees and cohesion of 1155 kPa was chosen. The elastic properties  $E$  and  $\nu$ , and the viscoplastic parameter,  $A$ , were the same as in the previous section.

Figure 5.14 shows the stress path for two values of  $\Delta t$  beyond  $\Delta t_{\text{max}}$ . As shown in this figure, stability was maintained even for a time step of  $9.4 \Delta t_{\text{max}}$ . As the time step was increased further, such that  $\Delta t = 14 \Delta t_{\text{max}}$ , error in the steady state solution resulted as stresses stopped inside the elastic region in one step. The results of this simulation reveal that if one were to use an accelerated solution scheme, numerical stability can be maintained but, depending on the magnitude of the accelerated time step beyond  $\Delta t_{\text{max}}$ , an incorrect steady state solution may be obtained. It should be noted that in this particular problem, stress redistribution did not occur since all stresses within the domain were the same. In the next chapter an example is

presented in which stress redistribution causes the elimination of the aforementioned steady state solution error when using an accelerated scheme. In particular, stresses that oscillate into the elastic region can later oscillate back into the plastic region due stress redistribution.

As was done previously in Section 5.3.1, the maximum time step was calculated from the equilibrium expression for an "associative" law. The ratio between the calculated time step,  $\Delta t_{\max}^{1D}$ , and the one based on Equation (4.17) is given by

$$\Delta t_{\max}^{1D} = \frac{2(1-\nu)(1-2\nu+\sin^2\phi)}{(1-2\nu)(1-2\sin\phi + \sin^2\phi)} \Delta t_{\max} \quad (5.14)$$

This equation reveals that the error between the actual and proposed maximum time step is dependent on Poisson's ratio and the material friction angle. As was already shown in Figure 5.14,  $\Delta t_{\max}^{1D}/\Delta t_{\max} = 9.4$  for  $\phi=30$  degrees and  $\nu=0.34$ . Figure 5.15 shows that for  $\nu=0.34$  and increasing friction angle, the difference between  $\Delta t_{\max}^{1D}$  and  $\Delta t_{\max}$  increases. Several finite element simulations were performed for various values of  $\phi$  and the results were as expected from Equation (5.14).

Similar comparisons were made by varying  $\nu$  and  $\phi$ . It was found that for low Poisson's ratio,  $\nu < 0.35$ ,  $\Delta t_{\max}^{1D}/\Delta t_{\max}$  was primarily dependent on  $\phi$ . As  $\nu$  increased beyond 0.35, the value of  $\Delta t_{\max}^{1D}/\Delta t_{\max}$  became dependent on both  $\nu$  and  $\phi$ , with the ratio increasing as  $\nu$  and  $\phi$  are increased.

The results of this section indicate how conservative the proposed stability criterion can be. By introducing the influence of level of constraint into the stability criterion, one should be able to obtain a more efficient time step size. As mentioned previously, the actual level of constraint is not known, a priori.

The next chapter deals with using the elastic-viscoplastic algorithm to solve plasticity problems. As will be shown, the stability criterion examined in the previous examples is related to the plastic strain increment.

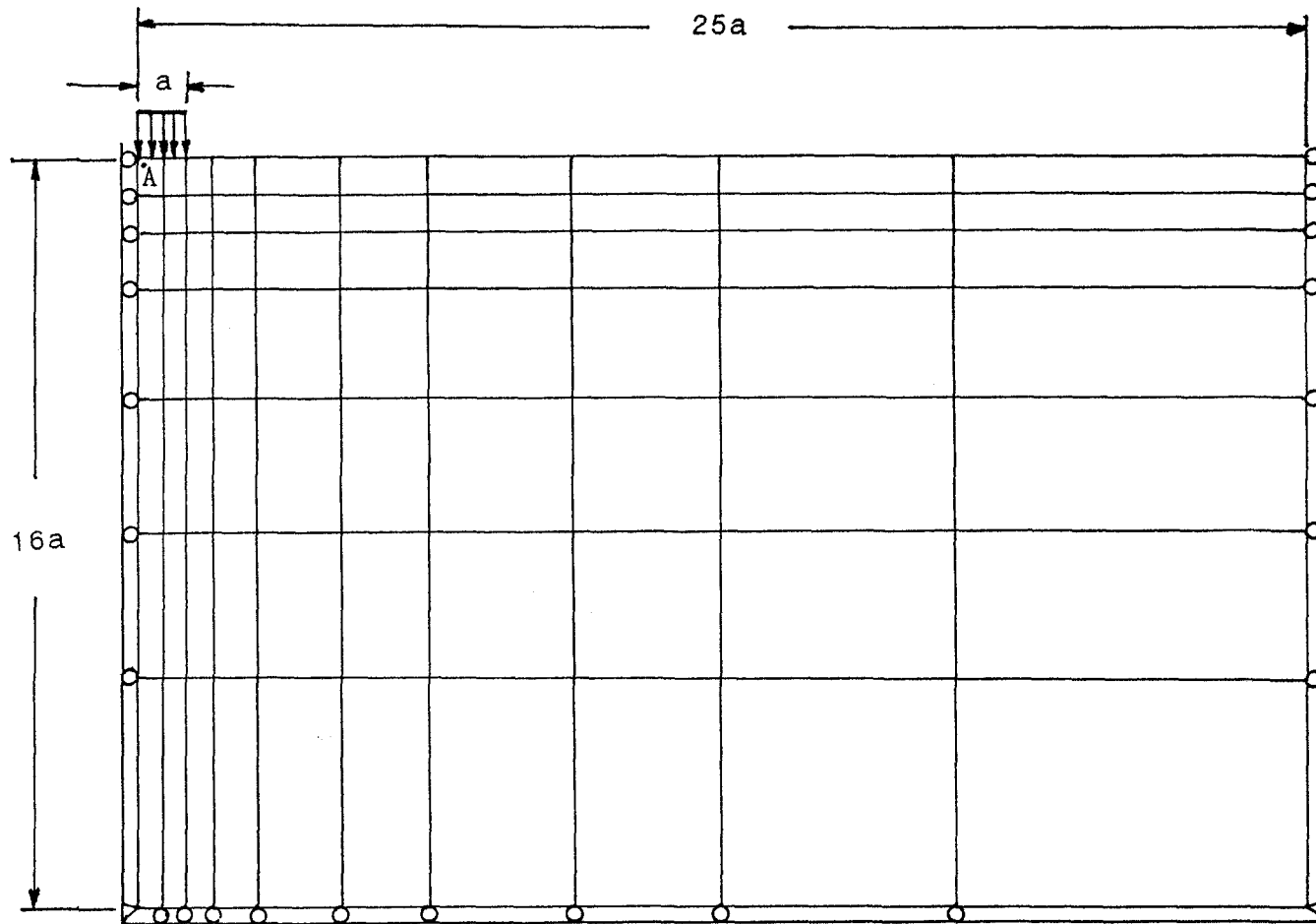


Figure 5.1 Plane Strain Strip Footing - 70 Element Grid

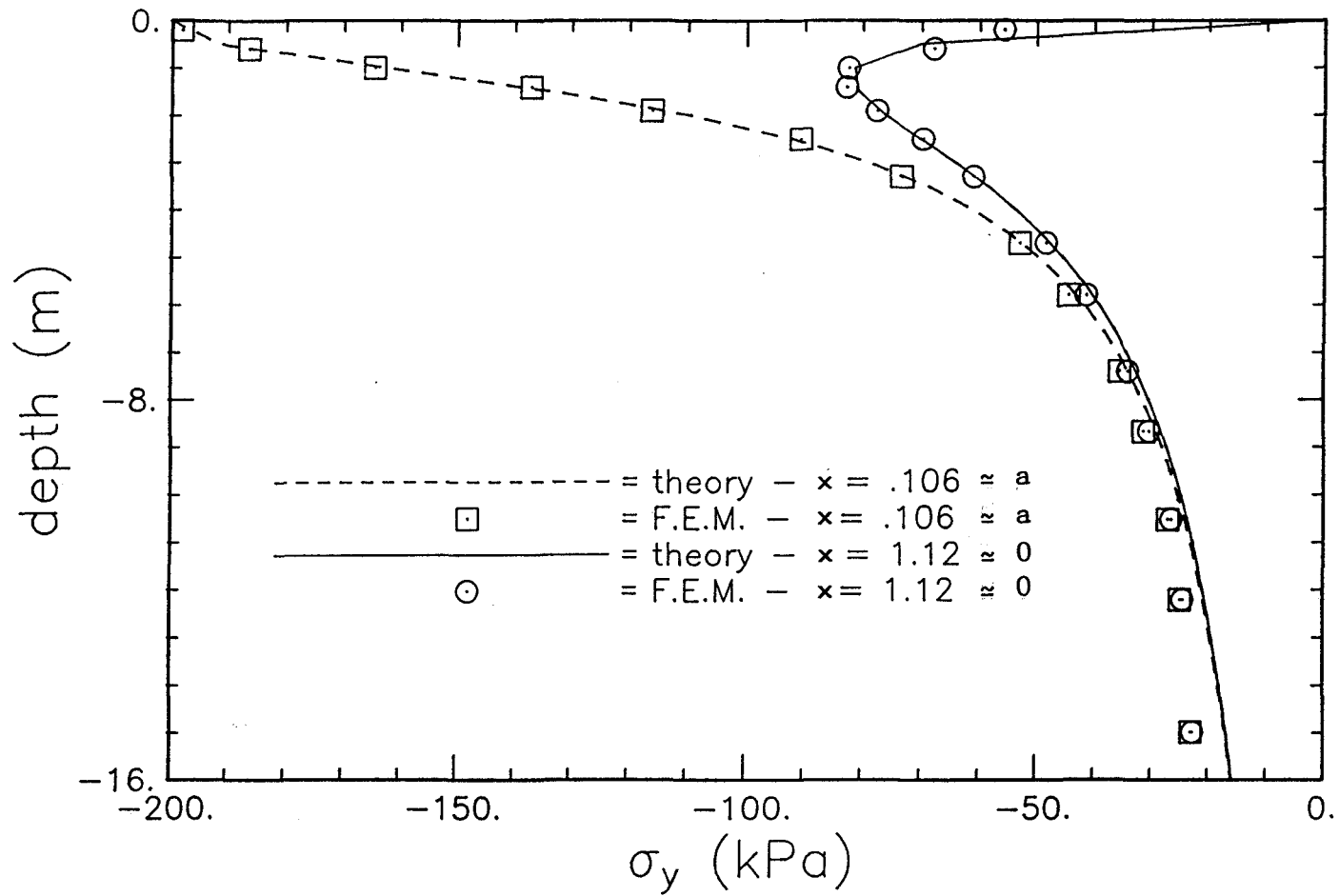


Figure 5.2 Vertical Stress Profile - Plane Strain Strip Footing

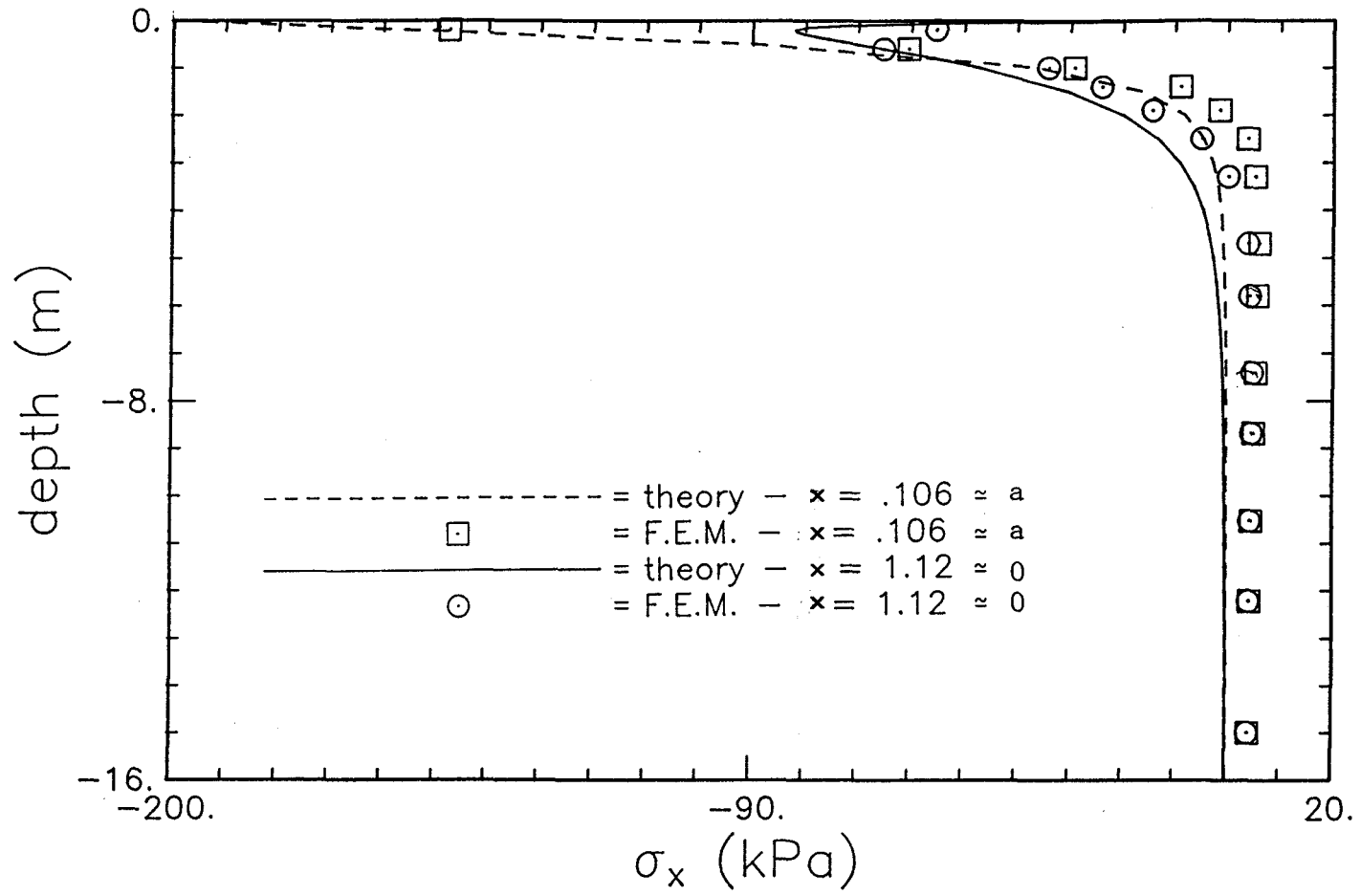


Figure 5.3 Horizontal Stress Profile - Plane Strain Strip Footing

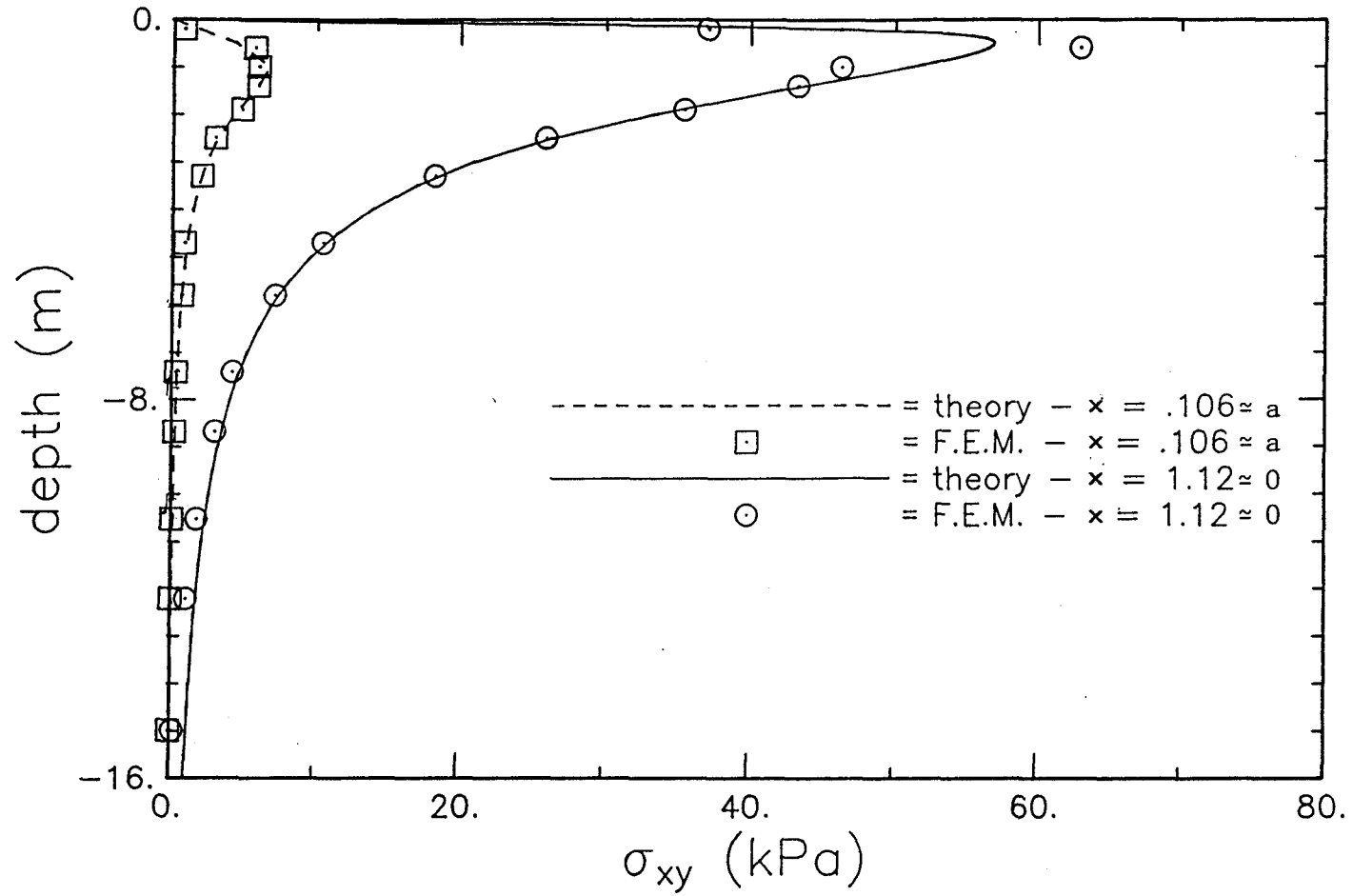


Figure 5.4 Shear Stress Profile - Plane Strain Strip Footing

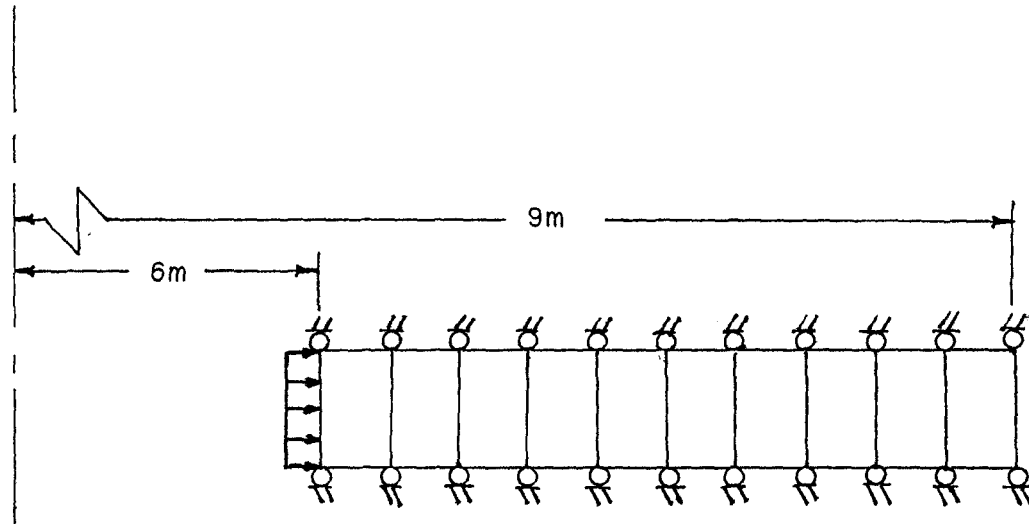


Figure 5.5 Axisymmetric Thick-Walled Cylinder - 10 Element Grid

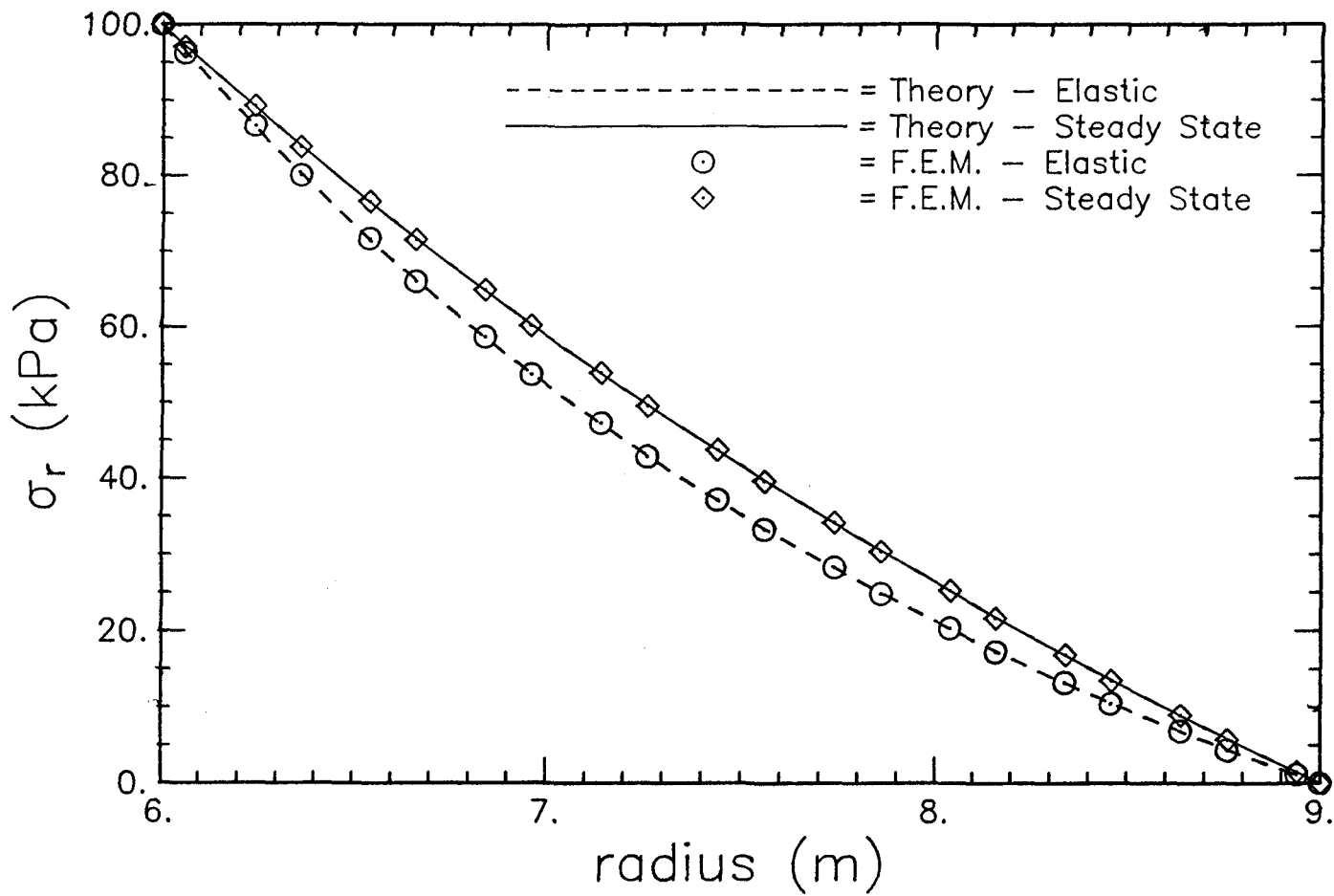


Figure 5.6 Axisymmetric Thick-Walled Cylinder  
Elastic and Steady State Creep Solution

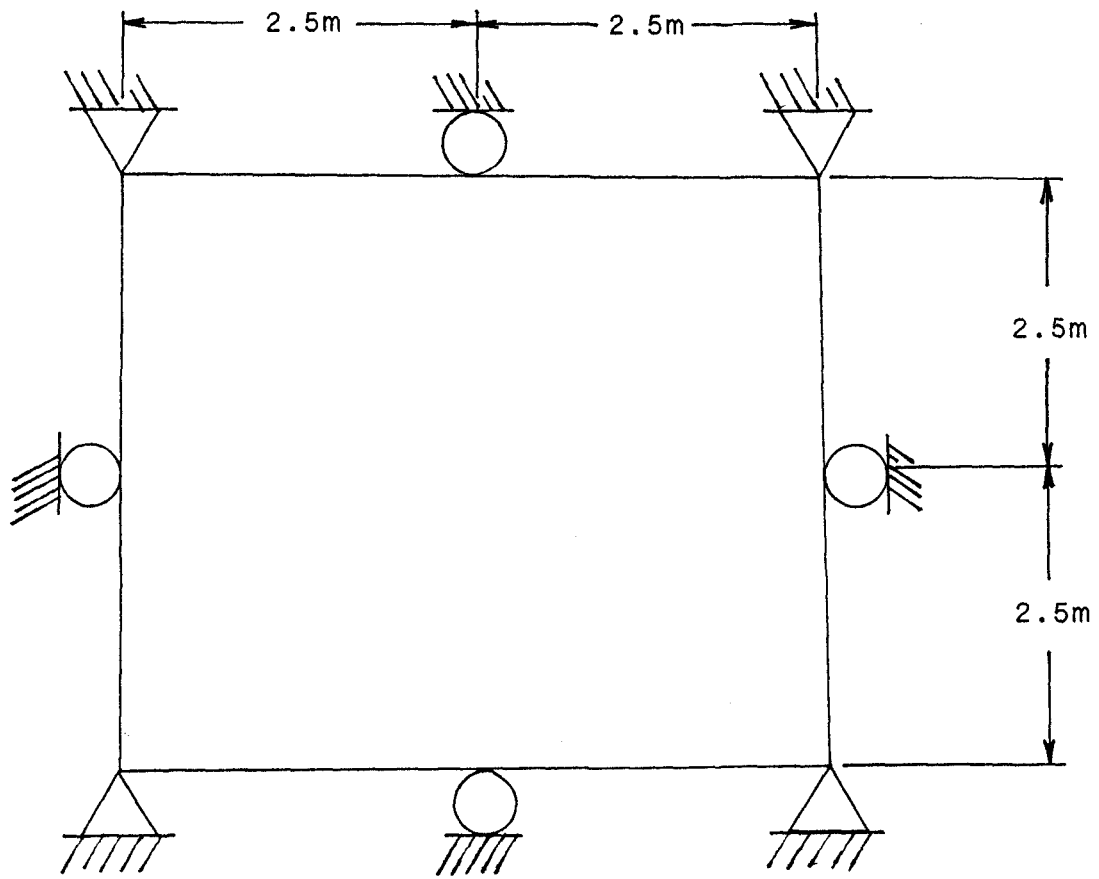


Figure 5.7 Stress Relaxation - 1 Element Grid

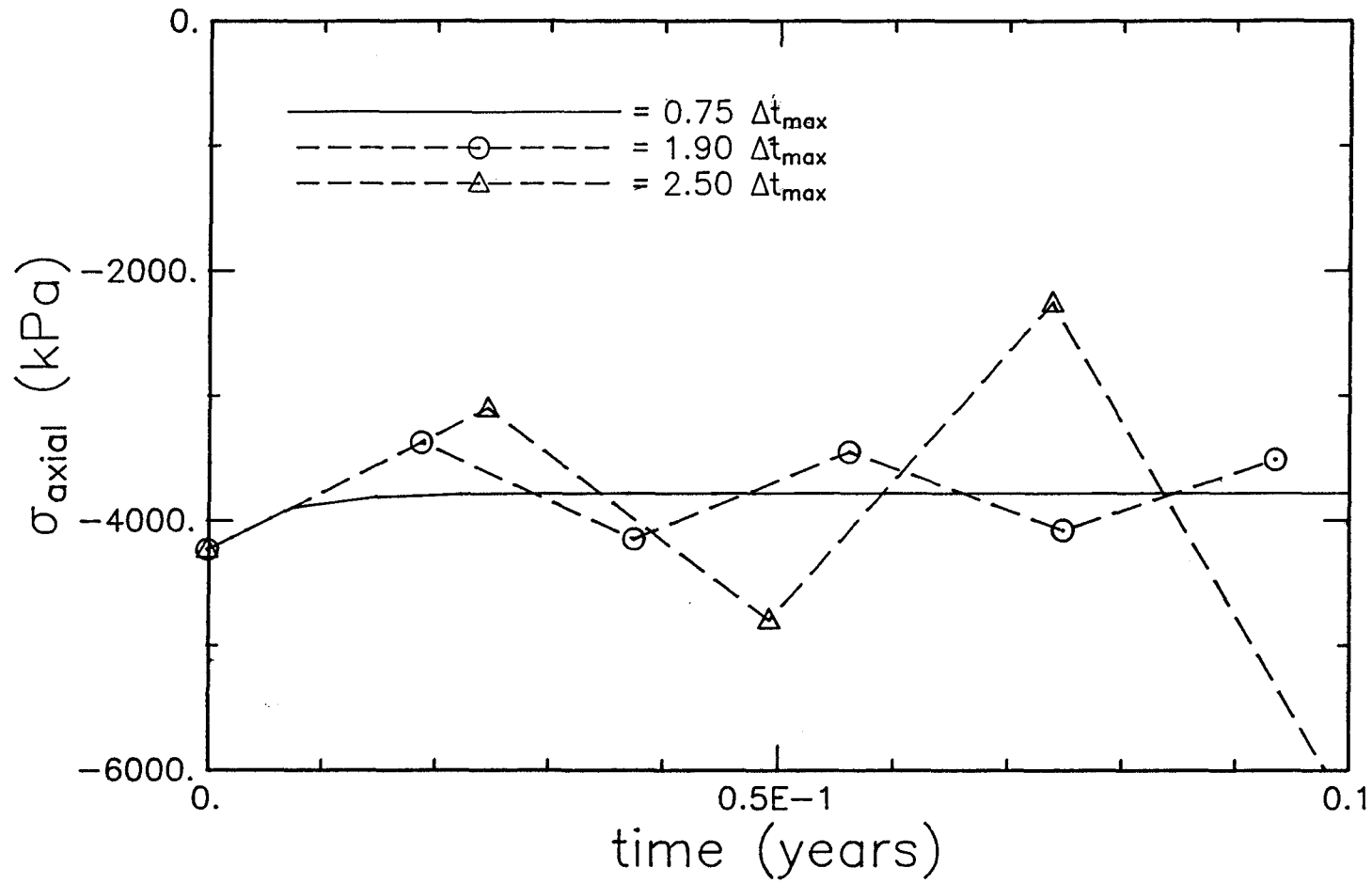


Figure 5.8 Instability Demonstration for Pure Stress Relaxation

$$\Delta \epsilon_a = \Delta \epsilon_r = \Delta \epsilon_\theta = 0 : m = 1$$

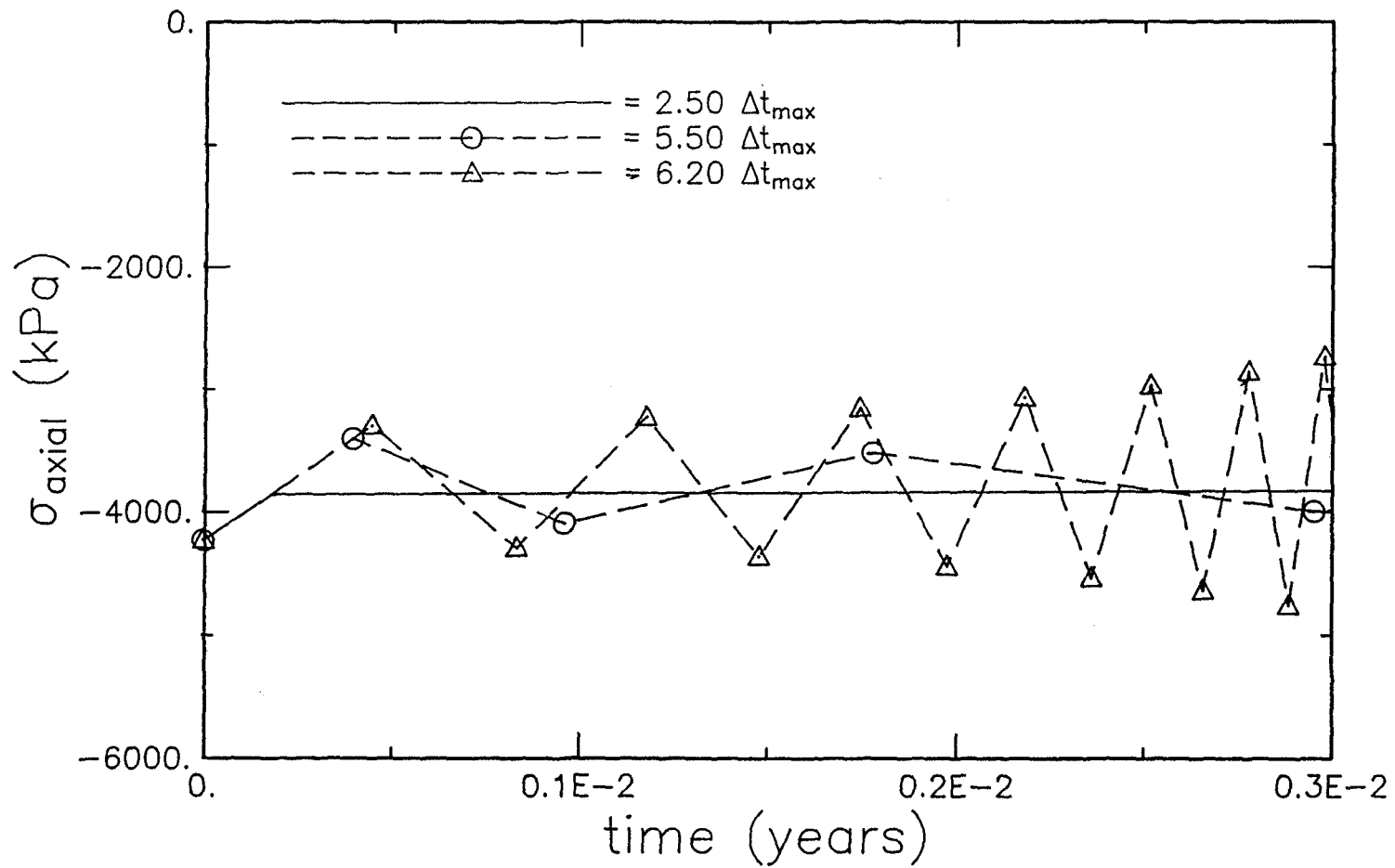


Figure 5.9 Instability Demonstration for Pure Stress Relaxation

$$\Delta \epsilon_a = \Delta \epsilon_r = \Delta \epsilon_\theta = 0 : m = 3$$

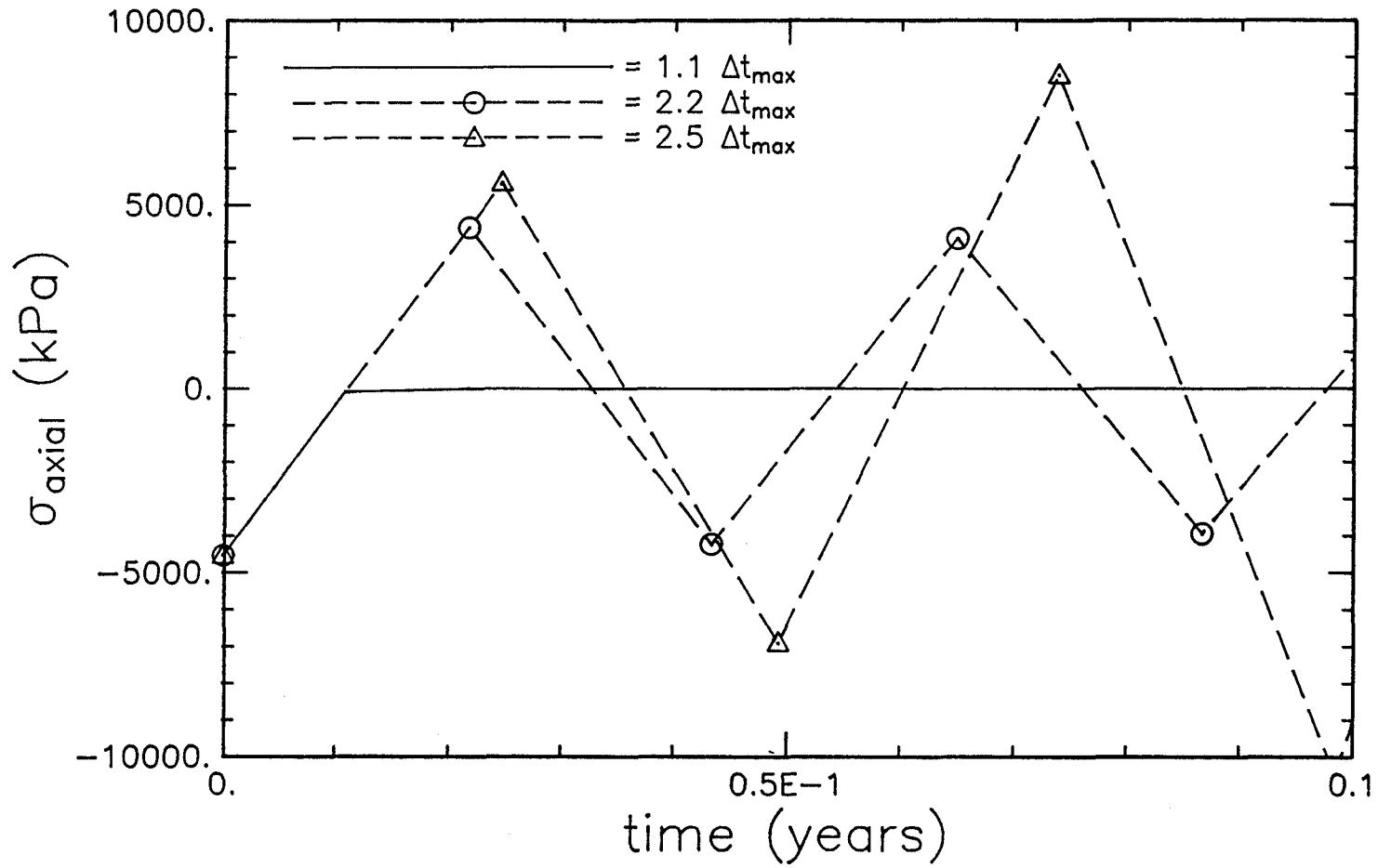


Figure 5.10 Instability Demonstration for Stress Relaxation

$$\Delta \epsilon_r \neq 0 : m = 1$$

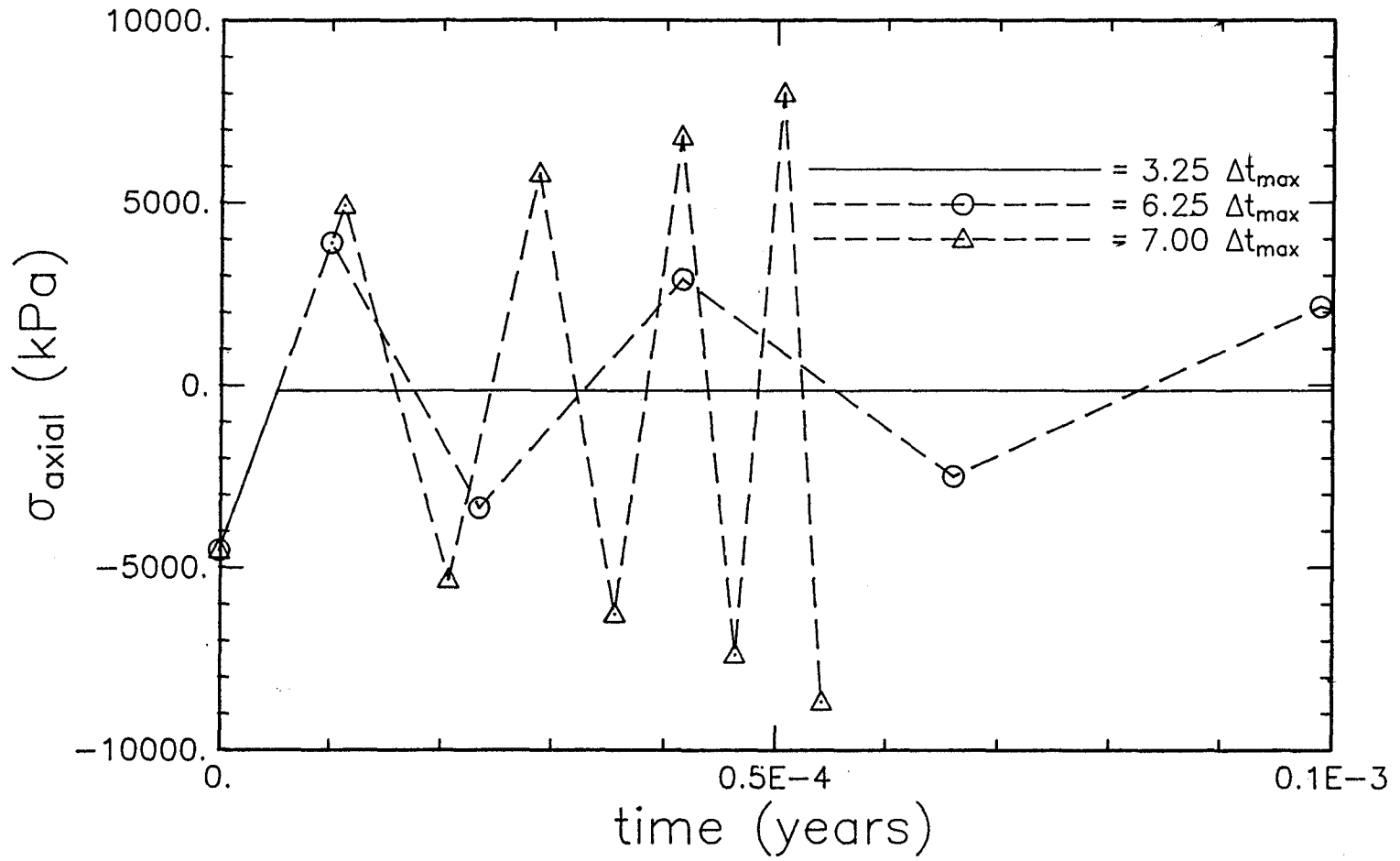


Figure 5.11 Instability Demonstration for Stress Relaxation

$\Delta \epsilon_r \neq 0 : m = 3$

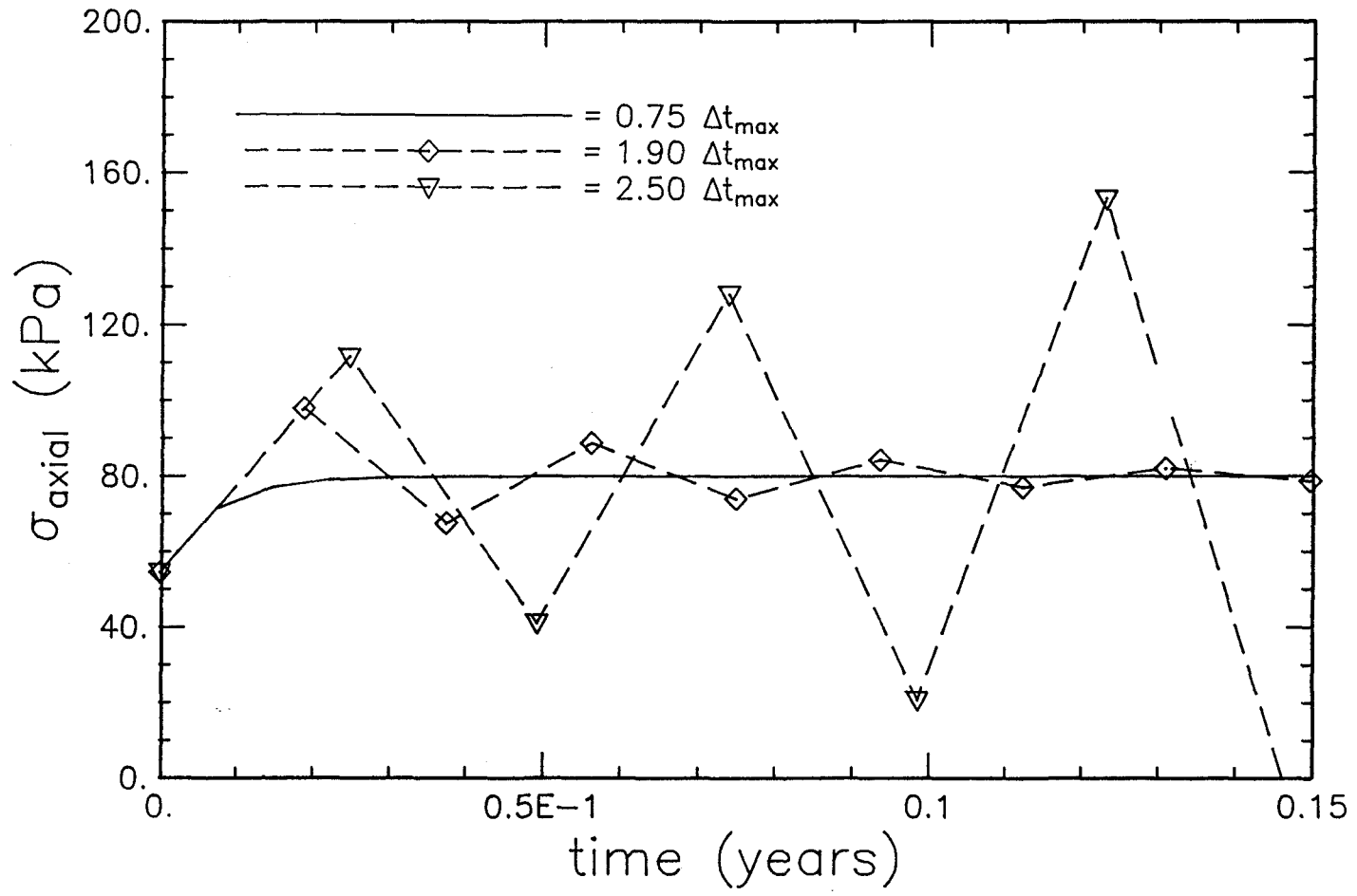


Figure 5.12 Instability Demonstration :  $m = 1$   
 Creep of Axisymmetric Thick Walled Cylinder

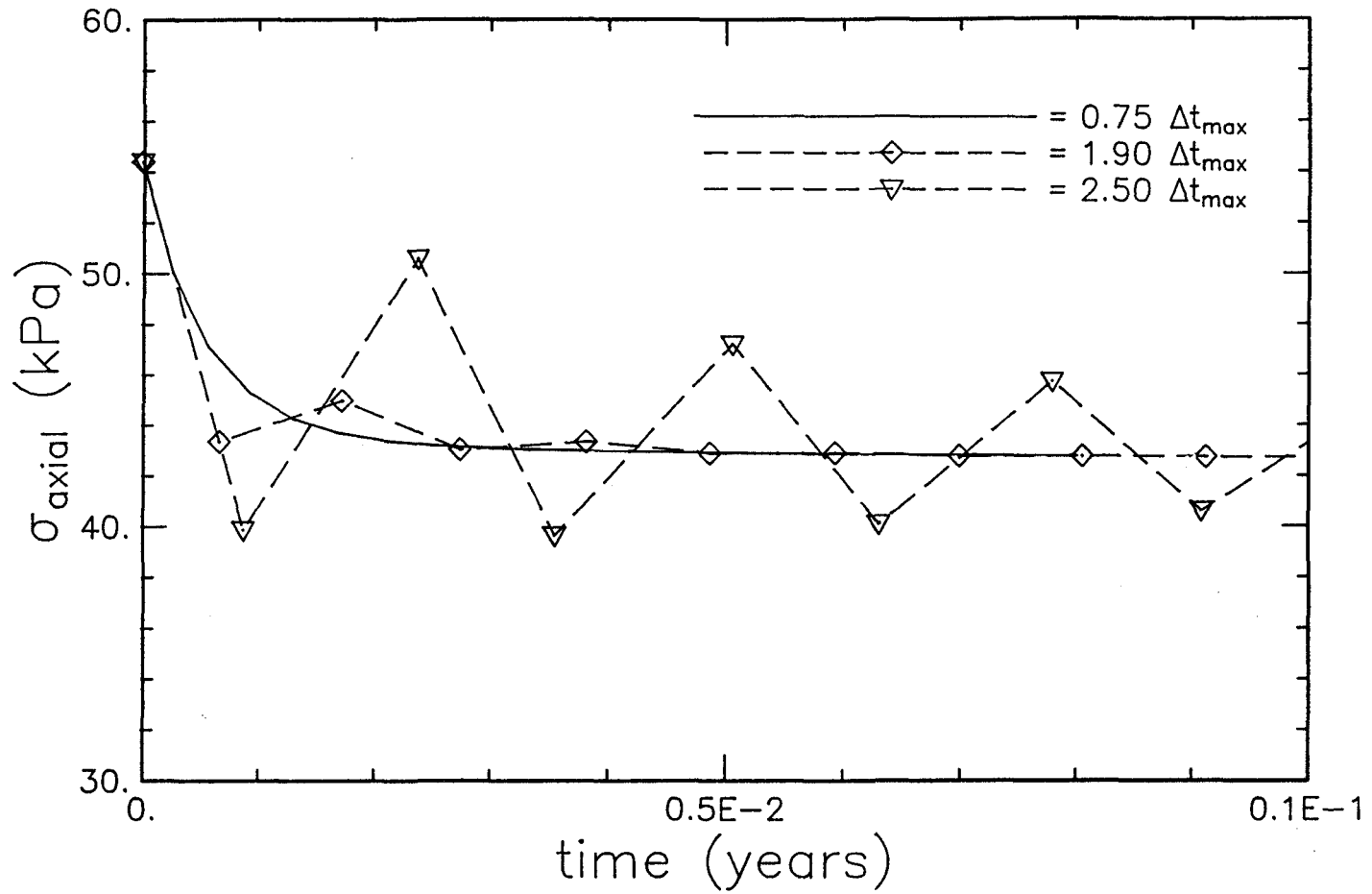


Figure 5.13 Instability Demonstration :  $m = 3$   
 Creep of Axisymmetric Thick Walled Cylinder

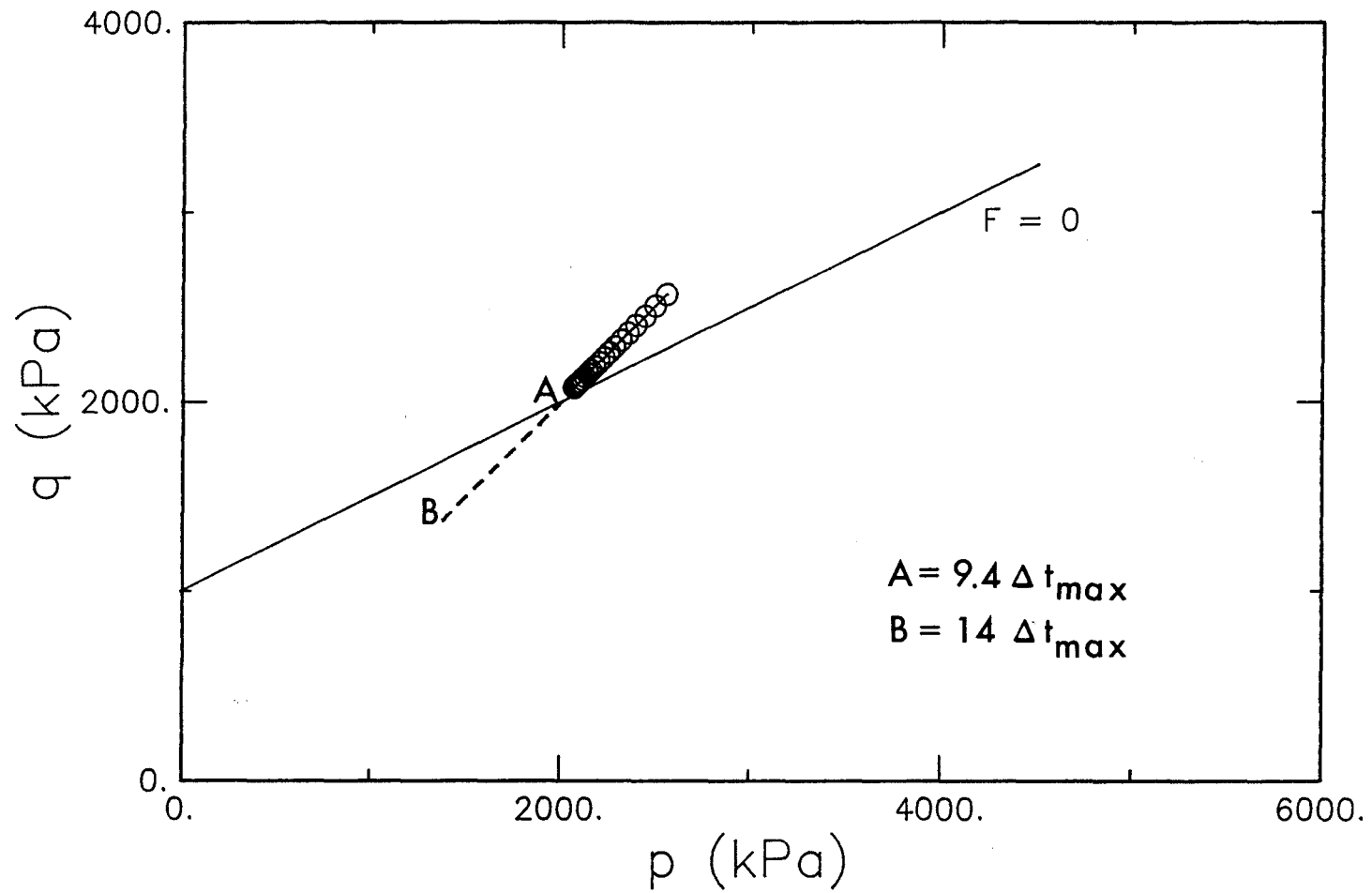


Figure 5.14 Instability Demonstration

Stress Relaxation : Mohr-Coulomb Plane Strain

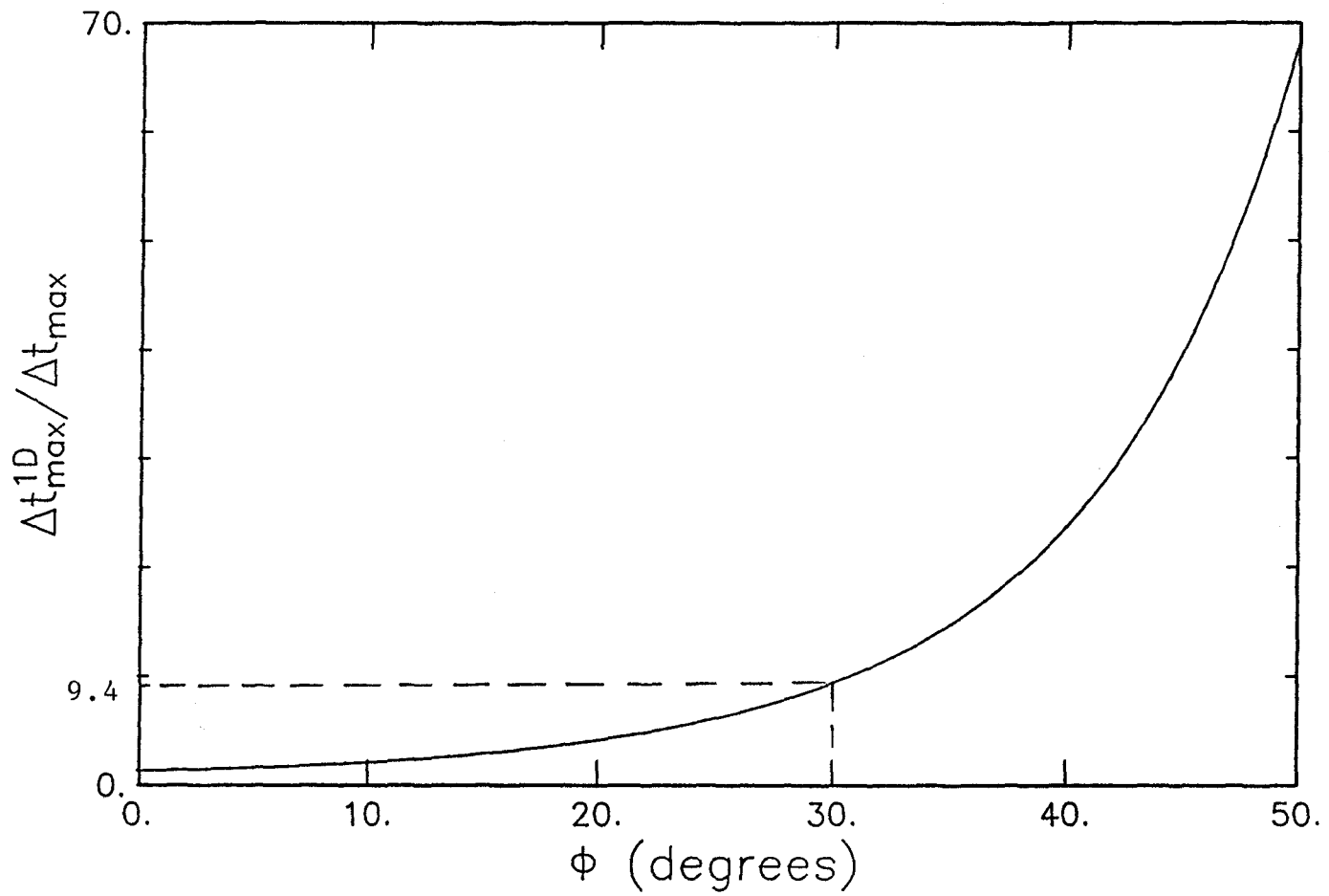


Figure 5.15 Level of Conservativeness Demonstrated ( $\nu=.34$ )  
 Stress Relaxation : Mohr-Coulomb Plane Strain

## CHAPTER 6

### ANALYSIS OF PLASTICITY PROBLEMS

#### 6.1 Plasticity Solutions via a Viscoplastic Approach

An important application of elastic-viscoplastic modelling is the generation of plasticity solutions [1]. Extensive work has been done in this area as mentioned in Chapter 1. In particular, it is usually implied that plasticity solutions correspond to steady state viscoplasticity solutions [1]. This section provides a brief comparison between the initial strain plasticity and viscoplasticity approaches. The presentation is restricted to non-hardening viscoplasticity.

In plasticity, the plastic strain rate vector is given by  $\Delta \epsilon^p = \beta \partial Q / \partial \sigma$  where  $\beta$  is obtained via a consistency condition and  $Q$  is a plastic potential function similar to that used for viscoplasticity (see, section 2.1). DeBorst and Vermeer [37], using an initial strain plasticity approach, indicated that the proportionality constant  $\beta$  can be expressed as follows:

$$\beta = \frac{\langle F(\sigma^e) \rangle}{H_e} \quad (6.1)$$

where  $H_e = (\partial F / \partial \sigma)^T D (\partial Q / \partial \sigma)$  and  $\sigma^e = \sigma_0 + D \Delta \epsilon$  is a fictitious stress used to evaluate  $\beta$ . Equation 6.1 is obtained by expanding  $F$ , using a truncated Taylor's series, about the fictitious stress  $\sigma^e$  rather than about a stress  $\sigma$  which sits on the yield surface.

Assuming a linear flow function and non-hardening, with the help of Equation (4.16) it may be shown that

$$\Gamma \Delta t_{\max} = \frac{\langle F(\sigma^e) \rangle}{H_e} = \beta \quad (6.2)$$

Equation (6.2) is identical to the scalar multiplier, given by Equation (6.1) for the initial strain plasticity approach. It is thus shown, taking into account the numerical equivalence of the initial stress and strain procedures, that the initial stress and viscoplasticity algorithms are the same provided that a linear, non-hardening flow function and  $\Delta t_{\max}$  are used in the viscoplastic algorithm. A further restriction is that the properties throughout the domain must be uniform since  $\Delta t_{\max}$  depends on the material properties. For the case of non-uniform properties,  $\Delta t_{\max}$  can be varied for each integration point.

One might expect that attempts to accelerate the convergence of such an initial strain plasticity approach by increasing the scalar multiplier through an acceleration factor could lead to poor predictions. Reference [28]

suggests using a deceleration factor when using initial strain plasticity.

The following sections are used to demonstrate the applicability of the viscoplastic algorithm to solve plasticity problems.

## 6.2 Plasticity Examples

In the examples given in Chapter 5, all results pertained to creep or viscoplasticity simulations where only one load increment was applied. The remaining set of examples were performed by incrementing load and allowing for an iterative initial strain loop within each load increment to obtain steady state solutions. The solutions to plasticity problems were generated by making use of the maximum time step based on Equation (4.16) as suggested in the previous section. The effect of violating this criterion in order to accelerate convergence to a steady state solution within each load increment is also briefly addressed.

The convergence criterion adopted in this thesis is an extension of a criterion suggested by Marques and Owen [11]. In their approach, they suggested that "convergence of the time stepping process to steady state conditions is monitored by requiring that the current value of the summation of the viscoplastic strain rates over the Gauss points be less than a specified percentage of that occurring in the first

time step of the load increment (typically less than 1.0%)". In the author's criterion, the summation of the strain rates were replaced by the square root of the summation of the square of all displacement increments, yielding

$$e = \left[ \frac{\sum_{j=1}^N (\Delta\delta_j \Delta\delta_j)_i}{\sum_{j=1}^N (\Delta\delta_j \Delta\delta_j)_0} \right]^{1/2} < e_{\text{MAX}} \quad (6.3)$$

where subscripts 0 and i correspond to displacements  $\delta_j$  in the first and the ith time increment, respectively. The number of degrees of freedom is represented by N, and j corresponds to the jth degree of freedom. A tolerance  $e_{\text{MAX}}$  of .1% was selected for the examples used in this thesis. If the solution failed to converge after 200 iterations, then it was assumed failure had occurred and the simulations were stopped.

In the following plasticity examples, a Tresca ( $\phi=0$ ) material description was assumed. A cohesion of 10 and 20 kPa was chosen for the first and second examples, respectively. The elastic and viscoplastic parameters were  $E=4800$  kPa,  $\nu=0.2$  and  $A=10^{-4} \text{ yr}^{-1} \text{ kPa}^{-1}$  for both examples. All simulations were completed using an associative flow law, ie.  $Q = F$ .

### 6.2.1 Thick Walled Cylinder

Since all shear stresses were zero, it was possible

to use the axisymmetric finite element discretization shown in Figure 5.5. In this case yielding was dependant on  $q = \sigma_r - \sigma_\theta$  where  $\sigma_r$  and  $\sigma_\theta$  are the tangential and radial stresses, respectively. The pressure,  $p_i$ , was incremented in steps of 0.1 kPa. The pressure was increased only after the iterative loop converged. In the example, the progression of plastic zones versus applied pressure were compared using a finite element and theoretical solution. The theoretical expression relating the progression of plastic zones to applied pressure is given in Reference [38] and is expressed as follows:

$$p_i/Y = \ln(c_i/r_i) + 1/2(1 - c_i^2/r_0^2) \quad (6.4)$$

where  $r_i$ ,  $r_0$  and  $c_i$  represent the inner, outer and yielded radii, respectively. The yield and applied stress are represented by  $Y = 2c$  and  $p_i$ , respectively. Figure 6.1 shows that the finite element solution compares well with the theoretical solution for the case where  $\Delta t = \Delta t_{\max}$ . Differences between the two are attributed to both the size of the load increments used and discretization. For  $\Delta t > \Delta t_{\max}$ , the finite element predictions deviate from the closed form solution, as anticipated. The deviation increases as the time step size is increased. A more thorough examination of the stresses at each iteration showed that some of the stresses that were plastic previous to convergence became elastic at convergence because of stress oscillations.

It is clear from this example, that in order to predict reasonable trends, the simulation must be carried out using time steps which do not exceed  $\Delta t_{\max}$ . With this in mind, the stability criterion suggested by Cormeau [15], ie.  $\Delta t < 2 \Delta t_{\max}$  ( =  $\Delta t_{\text{crit}}$  ), may not be strict enough.

### 6.2.2 Strip Footing Problem

The elastic-viscoplastic approach was also used to model an elasto-plasticity problem for the flexible strip footing configuration shown in Figure 5.1. The finite element solution is compared to the closed-form limiting equilibrium solution [39] ( $q_f=5.14c$ ) in Figure 6.2. In this figure, it is shown that the applied load versus vertical displacement, corresponding to point A shown in Figure 5.1, compares reasonably well for various values of  $\Delta t$ . The results once again demonstrate how conservative the stability criterion can be; since it is shown that a reasonable steady state response can be achieved even though the maximum time step ( $\Delta t_{\max}$ ) is exceeded by a factor of 4.

The effect of using a time step larger than  $\Delta t_{\max}$  during a particular loading increment on ( $\sigma_{11} - \sigma_{22}$ ) is shown in Figure 6.3. While the larger  $\Delta t$  is suitable for obtaining the plastic response, Figure 6.3 clearly shows that larger time steps are not suitable if details of a transient response

are required as would be the case for predicting true viscoplastic behaviour.

### 6.3 Summary of Examples

The purpose of the previous two examples was to study the applicability of the numerical stability criterion and to assess how sensitive numerical solutions are to time steps exceeding  $\Delta t_{\max}$ . Of course, for the problems of this chapter,  $\Delta t$  acted as a fictitious parameter controlling the size of the plastic strain step; ie. it was not a true measure of time. Problems involving more complex yield criterion and non-associative flow rules are left for future research work.

The examples clearly reveal that as time steps increase beyond  $\Delta t_{\max}$ , over-relaxation of stresses may occur, causing oscillatory behaviour. If the time step is increased beyond some critical value then stresses will redistribute in such a manner as to cause numerical instability.

The stability criterion developed in Chapter 4 was shown to be a conservative criterion for all examples used. Since the numerical stability criterion provides a "lower bound", some simulations resulted in an extremely overconservative maximum permissible time steps. The demonstrated levels of conservativeness associated with Equation (4.16) and therefore with that of Corneau help explain the success which some researchers have had when applying acceleration techniques[8].

Unfortunately, although accelerations schemes appear to work for some problems, there is no guarantee that they will be generally successful.

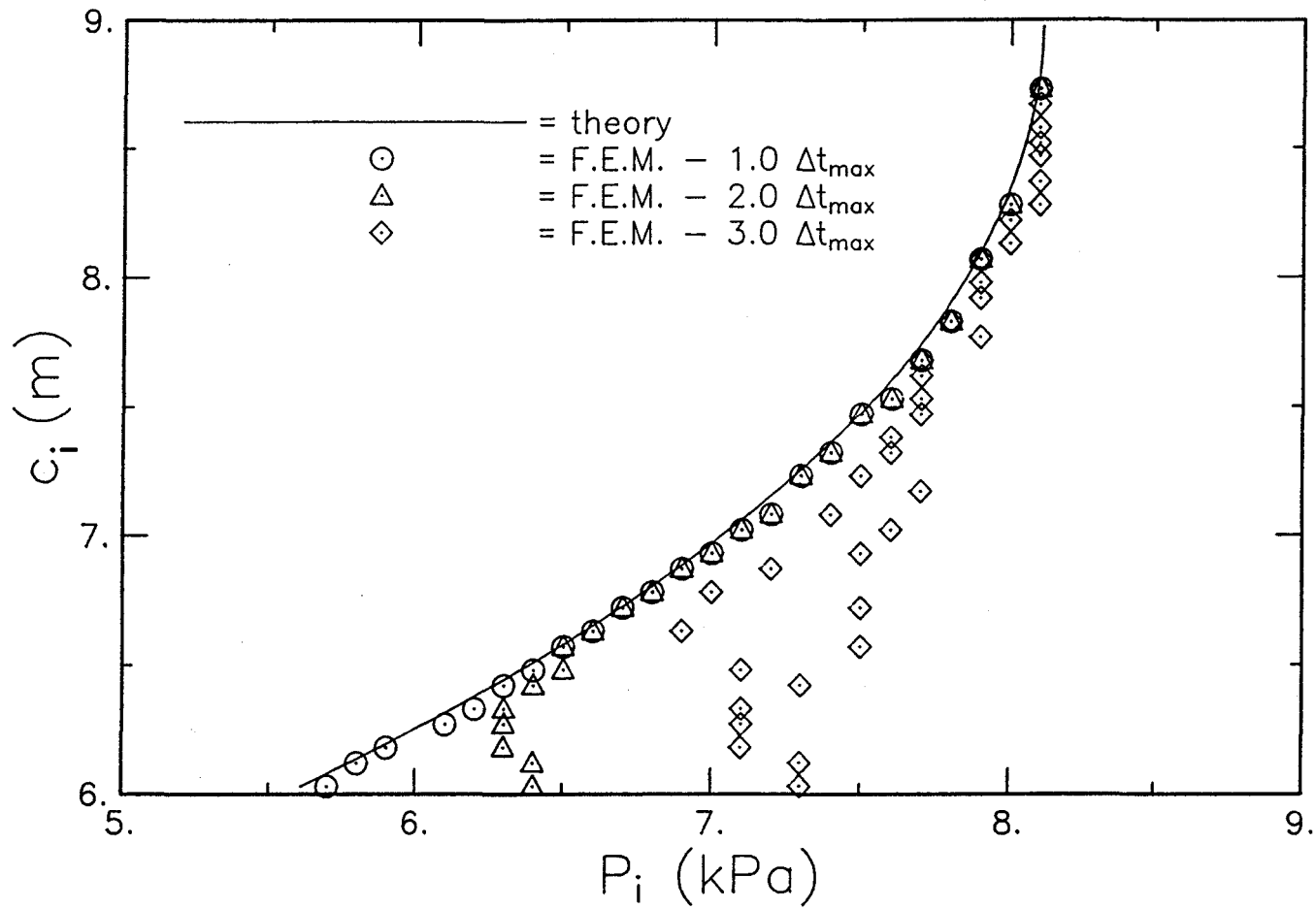


Figure 6.1 Progression of Plastic Zones : Instability  
 Axisymmetric Thick-Walled Cylinder - Tresca

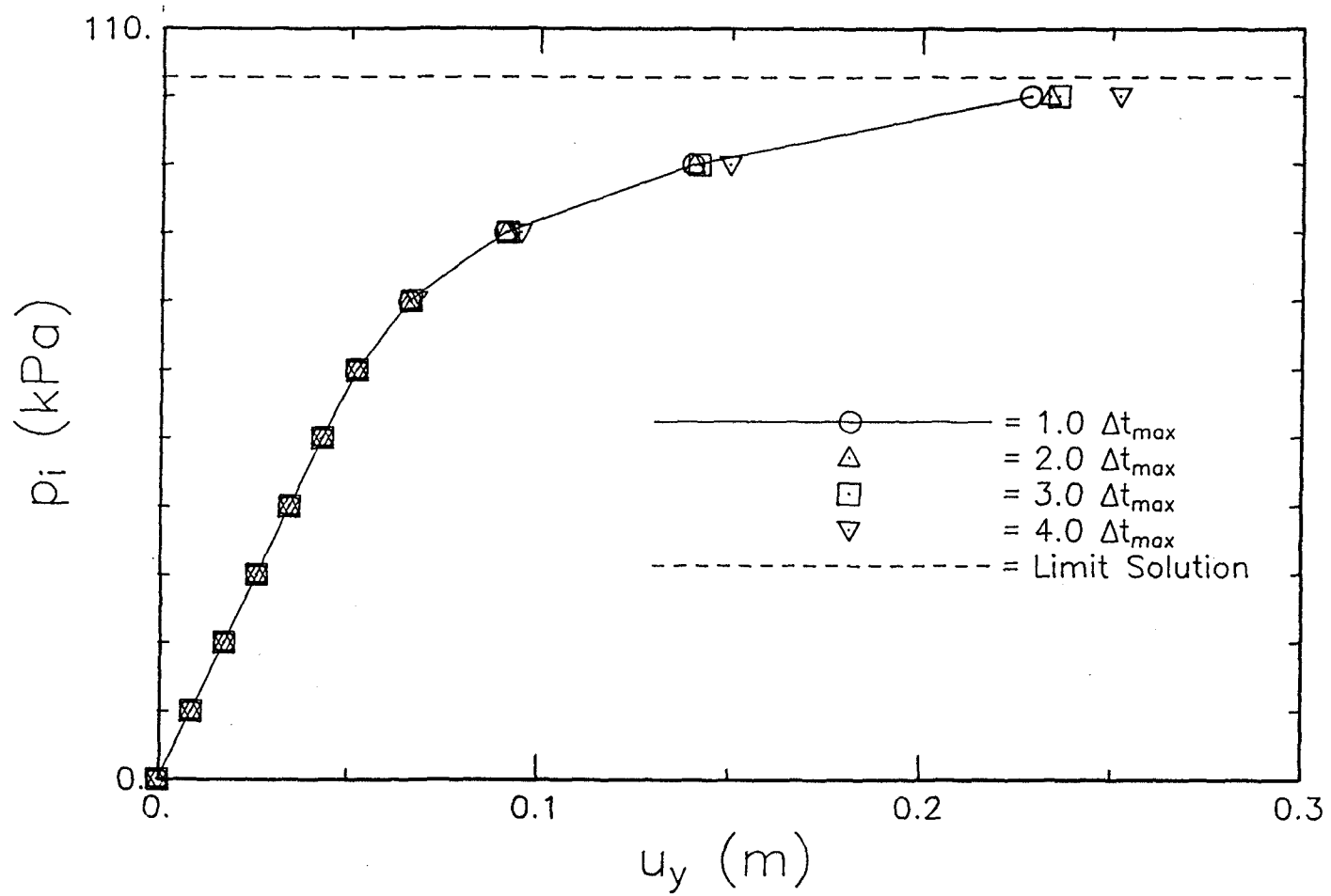


Figure 6.2 Surface Displacement at Center of Strip Footing  
Plane Strain Tresca - Instability Explored

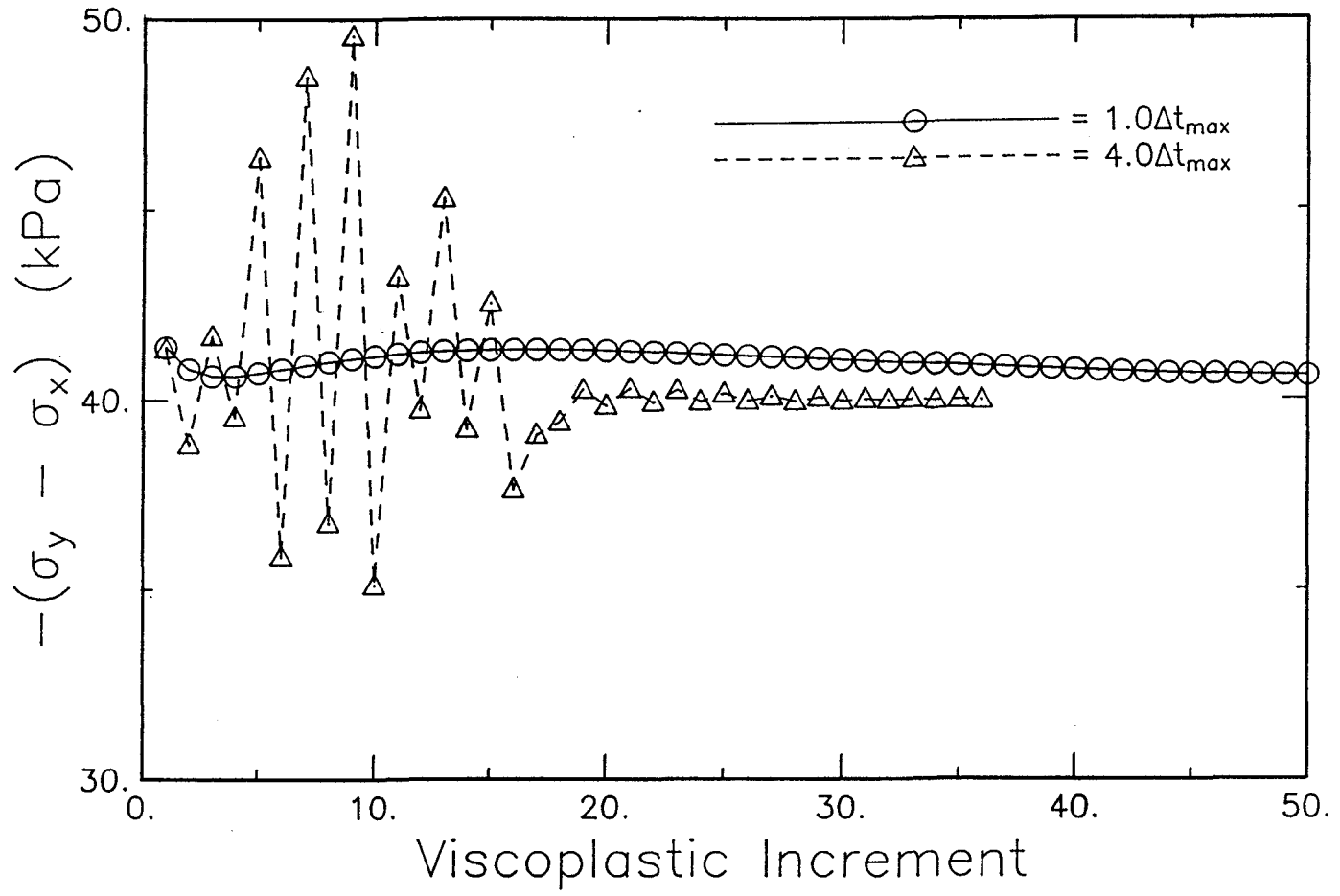


Figure 6.3 Stress Oscillations beneath center of Strip Footing  
 Tresca - 10th Load Increment : Yield = -40 kPa

## CHAPTER 7

### CONCLUSIONS AND RECOMMENDATIONS

#### 7.1 Conclusions

The main objective of this thesis was to extend Cormeau's work on numerical stability of explicit algorithms [15]. The simple, yet effective, approach was capable of accounting for work hardening and non-associative viscoplasticity which is not possible using Cormeau's approach.

The general expression for maximum permissible time-step is easily applied to a wide variety of material descriptions. For example, the derivation of the maximum permissible time step for the volumetric and deviatoric hardening models is presented in Appendix B. It was shown that the maximum permissible time step for the zero viscoplastic hardening and associative, Mohr-Coulomb, von Mises, Drucker-Prager and Tresca functions are the same as those of Cormeau [15]; that is, noting the relationship with Cormeau's stability criterion,  $\Delta t_{\text{crit}} = 2 \Delta t_{\text{MAX}}$ . Several examples were presented which show that the conservativeness of the criterion is highly problem dependent.

The stability criterion for  $\Delta t_{\text{MAX}}$  for an isotropic and

homogeneous material with no viscoplastic hardening and a linear power law was capable of producing an expression for plastic strain increment which is identical to that used for initial strain plasticity. It was shown that for some problems it is possible to accelerate convergence by using  $\Delta t > \Delta t_{\max}$  with very little difference in the converged solution.

The thesis provides a proposed implicit time-marching scheme which avoids matrix inversions, thereby improving computational efficiency. By making use of both the stability criterion and the implicit scheme, it should be possible to develop efficient implicit-explicit solvers for a much larger range of viscoplasticity laws than is currently possible.

In conclusion, the maximum time step derived from the traditional eigenvalue approach was based on only a few popular yield descriptions and limiting assumptions. At that time, there was not a high demand for the development of a numerical stability criteria for modelling more complex viscoplastic behaviour of materials. The need for an approach enabling the determination of stability criteria for more complex yield descriptions and hardening laws have increased due to more recent developments. It was the intent of this research to provide an approach which can be used to obtain a numerical stability criterion for these more complex viscoplastic descriptions.

## 7.2 Recommendations

Based on the work in this thesis several recommendations for further study can be made:

- (i) A comprehensive study of the proposed stability criterion applied to non-associative and work hardening viscoplasticity.
- (ii) Investigate the effectiveness of a criterion making use of Equation (4.15) which takes into account the level of constraint through  $\Delta\varepsilon$ ; i.e., using  $\Delta\varepsilon$  corresponding to the previous time increment.
- (iii) Applications of the stability criterion to a wider variety of material descriptions such as, volumetric and deviatoric hardening models.
- (iv) A thorough investigation of the proposed implicit time-marching scheme for viscoplasticity.

## APPENDIX A

### AN IMPLICIT VISCOPLASTIC FORMULATION

For certain forms of flow function, the maximum allowable time step may be very small, thereby making explicit time-marching schemes highly uneconomical. Unconditionally stable implicit schemes or implicit-explicit schemes can provide numerically efficient alternatives to the preferred explicit approach. For most analyses the objective is not to use very large time steps, but steps which are small enough to capture the essential trends of the phenomenon which one is trying to model, yet large enough to make the analysis economical. The main reason for the reluctance of adopting implicit schemes is the large computational effort, thus cost, associated with the inversion of the compliance matrix to obtain the elastic-viscoplastic tangent modulus matrix [32]. In the remainder of this appendix, an implicit scheme is developed which avoids the expensive matrix inversions.

In order to improve the numerical stability of the time-marching scheme, the influence of stress changes during the time increment must be taken into account. This may be accomplished by using Equation (4.14) and assuming that

$$\Delta \sigma = D [\Delta \epsilon - \Gamma \Delta t_n (\partial Q / \partial \sigma)] \quad (\text{A.1})$$

where  $\Gamma = \Gamma_{n+1}$  rather than  $\Gamma_n$  which was used for deriving the stability criterion. After substitution of Equation (A.1) into (4.14), one obtain

$$\Gamma_{n+1} = [ \Gamma_n + \Gamma' ( \partial F / \partial \sigma )^T D \Delta \epsilon ] / M \quad (A.2)$$

with

$$M = 1 + \Gamma' \Delta t_n (H_e + H_p) \quad (A.3)$$

Substitution of Equation (A.2) into (A.1) yields

$$\Delta \sigma_n = D^{vp} \Delta \epsilon_n - ( \Gamma_n / M ) \Delta t_n D ( \partial Q / \partial \sigma ) \quad (A.4)$$

where

$$D^{vp} = D [ I - ( \Gamma' / M ) \Delta t_n ( \partial Q / \partial \sigma ) ( \partial F / \partial \sigma )^T D ] \quad (A.5)$$

The tangent matrix given by Equation (A.5) resembles that obtained in plasticity formulations. In fact for  $\Delta t_n \rightarrow \infty$ , the plasticity tangent matrix is obtained exactly. The main difference between  $D^{vp}$  and the one developed by Kanachi et al. [2] is that the effect of stress change on the gradient vector  $\partial Q / \partial \sigma$  is not taken into account in Equations (A.4) and (A.5).

APPENDIX B  
NUMERICAL STABILITY OF DEVIATORIC AND  
VOLUMETRIC HARDENING MODELS

B.1 General

As mentioned in Chapter 4, the author is not familiar with any literature that provides a numerical stability criterion for the deviatoric and volumetric hardening models. In this appendix, the maximum permissible time step associated with both these material descriptions are presented for two-dimensional analysis. In the deviatoric concept, no hardening and a non-associative flow will be assumed. In the volumetric concept, it will be assumed that no hardening and an associative flow rule exists.

B.1.1 Deviatoric model

In this example a non-associative law shall be assumed. The yield function and plastic potential may be given in the particular form:

$$F(p, q, \epsilon_q^p) = q - \eta p = 0 \quad (\text{B.1})$$

$$Q(p, q) = q + \eta_c p \ln(p/p_0) = 0 \quad (\text{B.2})$$

in which  $\eta$  is assumed to be a hyperbolic function of plastic deviatoric strain  $\epsilon_q^p$

$$\eta(\epsilon_q^p) = \eta_f \frac{\epsilon_q^p}{L + \epsilon_q^p} \quad (\text{B.3})$$

Here  $\eta_f$ ,  $\eta_c$  represent stress ratio  $q/p$  at failure and zero dilatancy state, respectively and  $L$  is a material constant.

Assuming a Mohr-Coulomb plane strain representation:

$$q = [(\sigma_{11} - \sigma_{22})^2 + 4\sigma_{12}^2]^{1/2} \quad (\text{B.4})$$

$$p = (\sigma_{11} + \sigma_{22}) \quad (\text{B.5})$$

From Equations (B.1), (B.2), (B.4) and (B.5) we get:

$$\begin{aligned} \partial F / \partial \sigma_{11} &= (\sigma_{11} - \sigma_{22}) / q + \eta \\ \partial F / \partial \sigma_{22} &= -(\sigma_{11} - \sigma_{22}) / q + \eta \\ \partial F / \partial \sigma_{12} &= 4\sigma_{12} / q \end{aligned} \quad (\text{B.6})$$

and

$$\begin{aligned} \partial Q / \partial \sigma_{11} &= (\sigma_{11} - \sigma_{22}) / q + \eta_c - \eta \\ \partial Q / \partial \sigma_{22} &= -(\sigma_{11} - \sigma_{22}) / q + \eta_c - \eta \\ \partial Q / \partial \sigma_{12} &= 4\sigma_{12} / q \end{aligned} \quad (\text{B.7})$$

The maximum time step  $\Delta t_{\max} = 1 / [\Gamma' (H_e + H_p)]$ , where

$H_e = (\partial F / \partial \sigma)^T D (\partial Q / \partial \sigma)$ ,  $H_p$  is a viscoplastic hardening parameter

(assumed equal to zero) and  $\Gamma'$  is defined in Chapter 4. Substitution of Equations (B.6), (B.7) and the plane strain elastic matrix

$$D = E_1 \begin{vmatrix} 1 & \nu/(1-\nu) & 0 \\ \nu/(1-\nu) & 1 & 0 \\ 0 & 0 & (1-2\nu)/[2(1-\nu)] \end{vmatrix} \quad (\text{B.8})$$

where  $E_1 = E(1-\nu)/[(1+\nu)(1-2\nu)]$  into the expression for  $H_e$  yields

$$H_e = E_1 [1-2\nu + 2\eta(\eta_c - \eta)] \quad (\text{B.9})$$

Substituting Equation (B.9) into the expression for maximum time step gives

$$\Delta t_{\max} = \frac{1}{E_1 [1-2\nu + 2\eta(\eta_c - \eta)]} \quad (\text{B.10})$$

### B.1.2 Volumetric model

For this model, the yield function may be assumed in the particular form:

$$F(p, q, \varepsilon_v^p) = (p-a_0)^2 + q^2/\eta_f^2 - a_0^2 = 0 \quad (\text{B.11})$$

in which  $\eta_f$  represents the stress ratio  $q/p$  at critical state.

From Equations (B.11), (B.4) and (B.5) we get:

$$\begin{aligned}\partial F / \partial \sigma_{11} &= 2(\sigma_{11} + \sigma_{22} - a_0) + 2(\sigma_{11} - \sigma_{22}) / \eta_f^2 \\ \partial F / \partial \sigma_{22} &= 2(\sigma_{11} + \sigma_{22} - a_0) - 2(\sigma_{11} - \sigma_{22}) / \eta_f^2 \\ \partial F / \partial \sigma_{12} &= 8\sigma_{12} / \eta_f^2, \quad \partial F / \partial \sigma_{33} = 0\end{aligned}\tag{B.12}$$

Substitution of the Equations (B.12) and the plane strain elastic matrix into the expression for  $H_e$ , and assuming an associative law yields

$$H_e = 8E_1 [(p - a_0)^2 + q^2(1 - 2\nu) / \eta_f^4]\tag{B.13}$$

Substituting Equation (B.9) into the expression for maximum time step (noting that  $H_p$  is assumed equal to zero) gives

$$\Delta t_{\max} = \frac{1}{8\Gamma'E_1 [(p - a_0)^2 + q^2(1 - 2\nu) / \eta_f^4]}\tag{B.14}$$

Thus, a maximum permissible time step is obtained for the deviatoric and volumetric models applicable to plane strain. The introduction of viscoplastic hardening into the formulation is left for the reader.

## APPENDIX C

### DERIVATION DETAILS OF NUMERICAL STABILITY EXPRESSIONS

#### C.1 General

To obtain an expression for maximum time step using Equation (4.16) requires several steps too lengthy to be shown in the main body of the thesis. Nevertheless, details of the derivations leading to an expression for maximum time step for the von Mises and Mohr-Coulomb yield functions are contained in this appendix.

##### C.1.1 Numerical Stability for Mohr-Coulomb Yield Function

The derivation of the stability criterion for the Mohr-Coulomb yield description is based on the assumption of plane strain, no hardening, ie.  $H_p=0$ , and a non-associative law. The yield and plastic potential functions are given by equations (2.14) and (2.15), respectively. Using these Equations, the corresponding expressions can be obtained:

$$\begin{aligned}\partial F / \partial \sigma_{11} &= (\sigma_{11} - \sigma_{22}) / q + \sin \phi \\ \partial F / \partial \sigma_{22} &= -(\sigma_{11} - \sigma_{22}) / q + \sin \phi \\ \partial F / \partial \sigma_{12} &= 4 \sigma_{12} / q\end{aligned}\tag{C.1}$$

and

$$\begin{aligned}
\partial Q / \partial \sigma_{11} &= (\sigma_{11} - \sigma_{22}) / q + \sin \psi \\
\partial Q / \partial \sigma_{22} &= -(\sigma_{11} - \sigma_{22}) / q + \sin \psi \\
\partial Q / \partial \sigma_{12} &= \partial F / \partial \sigma_{12}
\end{aligned}
\tag{C.2}$$

The plane strain material matrix was given previously in Appendix B.

By substituting (C.1), (C.2) and the plane strain material matrix into  $H_e = (\partial F / \partial \sigma)^T D (\partial Q / \partial \sigma)$  yields the following:

$$H_e = 2E [(1-2\nu) + \sin \phi \sin \psi] / [(1-2\nu)(1+\nu)] \tag{C.3}$$

By using Equation (2.3) which assumes a power law for creep,  $\Gamma' = \partial \Gamma / \partial F$  can be expressed as follows:

$$\Gamma' = m F^{n-1} \tag{C.4}$$

which yields the following expression for maximum time step based on Equation (4.16) which is given in Section 4.5:

$$\Delta t_{\max} = \frac{(1+\nu)(1-2\nu)}{2EAmF^{n-1} (1-2\nu + \sin \phi \sin \psi)} \tag{C.5}$$

It should be noted here that for the Tresca case  $\phi = \psi = 0$  and the corresponding expression for maximum time step reduces to:

$$\Delta t_{\max} = \frac{(1+\nu)}{2EA_m F^{n-1}} \quad (\text{C.6})$$

### C.1.2 Numerical Stability for a von Mises Yield Description

The derivation of the expression for maximum time step for the von Mises yield description is based on the assumption of axial symmetry or plane strain, no hardening and an associative law. The following expression is obtained from the yield function given by Equation (2.9):

$$\partial F / \partial \sigma = 3 / [2(3J_2^1)^{1/2}] \langle s_{11}, s_{22}, 2s_{12}, s_{33} \rangle^T \quad (\text{C.7})$$

By substituting Equation (C.7) and the material matrix :

$$D = E_1 \begin{vmatrix} 1 & \nu/(1-\nu) & 0 & \nu/(1-\nu) \\ \nu/(1-\nu) & 1 & 0 & \nu/(1-\nu) \\ 0 & 0 & (1-2\nu)/[2(1-\nu)] & 0 \\ \nu/(1-\nu) & \nu/(1-\nu) & 0 & 1 \end{vmatrix} \quad (\text{C.8})$$

where  $E_1 = E(1-\nu)/[(1+\nu)(1-2\nu)]$  into the expression for  $H_e$  yields

$$H_e = 3E / [2(1+\nu)] \quad (\text{C.9})$$

Substituting Equation (C.9) into the expression for maximum

time step gives

$$\Delta t_{\max} = \frac{2(1+\nu)}{3EA_m \sigma_e^{n-1}} \quad (\text{C.10})$$

where  $\sigma_e = (3J_2^I)^{1/2}$ .

## APPENDIX D

### CLOSED-FORM 1-D STABILITY CRITERION

Consider the geometric configuration used for the stress relaxation problem constrained in the axial direction; ie.  $\Delta\epsilon_{22} = 0$ . This problem can be reduced to one dimension and the resulting stability criterion applicable to an explicit time stepping scheme can be obtained. The approach for obtaining the corresponding maximum permissible time step is summarized in this appendix.

Owing to the boundary conditions associated with this problem, only  $\sigma_{22}$  stresses change. Hooke's Law relating total stresses increments to elastic strain increments can be expressed as follows:

$$\Delta\sigma_{22} = E \Delta\epsilon_{22}^e \quad (D.1)$$

where E is the elastic modulus. The consistency condition relating elastic and viscoplastic strain increments (noting that the total strain increment  $\Delta\epsilon_{22} = 0$ ) is expressed as follows:

$$\Delta\epsilon_{22}^e = -\Delta\epsilon_{22}^{VP} \quad (D.2)$$

For a von Mises material the viscoplastic strain increment is

$$\Delta \epsilon_{ij}^{VP} = 3/2 A \sigma_e^{n-1} s_{ij} \Delta t \quad (D.3)$$

Since only  $\sigma_{22}$  stresses exist, the second stress deviators is given as  $s_{22} = 2/3\sigma_{22}$ . Substitution of  $s_{22}$  into (D.3) gives

$$\Delta \epsilon_{22}^{VP} = A \sigma_e^{n-1} \sigma_{22} \Delta t \quad (D.4)$$

which when substituted into Equation (D.1) gives

$$\sigma_{22} = -EA \sigma_e^{n-1} \sigma_{22} \Delta t \quad (D.5)$$

Using an explicit finite difference approximation, such that  $\sigma^{n+1} = \sigma^n + \Delta \sigma^n$ , yields

$$\sigma_{22}^{n+1} = \sigma_{22}^n (1 - EA \sigma_e^{n-1} \Delta t) \quad (D.6)$$

In order to obtain  $\Delta t_{\max}$ , the maximum step size must be chosen such that oscillations are suppressed. The resulting maximum time step is as follows:

$$\Delta t_{\max}^{1D} = \frac{1}{AE \sigma_e^{n-1}} \quad (D.7)$$

## REFERENCES

- [1] Zienkiewicz, O.C. and Corneau, I.C., Viscoplasticity -plasticity and creep in elastic solids - a unified numerical solution approach, Int. J. Num. Meth. Eng. 1974, 8, 821-845.
- [2] Kanchi, M.B., Zienkiewicz, O.C., and Owen, D.R.J., The visco-plastic approach to problems of plasticity and creep involving geometric non-linear effects, Int. J. Num. Meth. Engng., 1987, 12, 169-181.
- [3] Argyris, J.H., St. Doltsinis, J. and Kleiber, M., Incremental formulation in nonlinear mechanics and large strain elasto-plasticity -- natural approach, part II., Computer Methods in Applied Mechanics and Engineering, 1987, Vol. 14, p. 259-294.
- [4] Argyris, J.H., Vas, L.E. and Willam, K.J., Improved solution methods for inelastic rate problems, Computer Methods in Applied Mechanics and Engineering, 1978, 16, p. 231-277.
- [5] Zienkiewicz, O.C., and Corneau, I.C., Visco-plasticity solution by finite element process. Archives of Mechanics (Warszawa), 1972, 24, 5-6, p. 873-889.
- [6] Klee, K.-D. and Paulun, J., On numerical treatment of large elastic-viscoplastic deformations. Archives of Mechanics (Warszawa), 1980, 32, p. 334-345.
- [7] Telles, J.C.F., and Brebbia, C.A., Elastic/viscoplastic problems using boundary elements. Int. J. Mech. Sci., 1982, Vol. 24, No. 10, p. 605-618.
- [8] Owen, D.R.J., and Damjanic, F. Viscoplastic analysis of solids: Stability Considerations. In; Recent Advances in Non-Linear Computational Mechanics, Ed. Hinton, E., Owen, D.R.J., and Taylor, C., Pineridge Press, 1982, Ch. 8, p. 224-254.
- [9] Zienkiewicz, O.C., Humpheson, C., and Lewis, R.W., Associated and non-associated visco-plasticity and plasticity in soil mechanics, Geotechnique, 1975, Vol. 25, No. 4, p. 671-689.

- [10] Argyris, J.H., Doltsinis, J.St. and Kleiber, M., Incremental formulation in nonlinear mechanics and large strain elasto-plasticity - natural approach. Part II, Computer Methods in Applied Mechanics and Engineering, 1978, v. 14, p. 259-294.
- [11] Marques, J.M.M.C. and Owen, D.R.J., Implicit-explicit time integration in quasi-static elastoviscoplasticity using finite and infinite elements, Computer Methods in Applied mechanics and Engineering, 1984, 42, p.167-182.
- [12] Damjanic, F., Owen, D.R.J., Implicit time integration of elasto-viscoplastic solids subject to the Mohr-Coulomb yield criterion, Int. J. Num. Meth. Engng., 1982, 18, p. 1873-1881.
- [13] Benallal, A., Structural analysis in quasi-static elasto-viscoplasticity. Engineering Computation, 1986, 3, p. 323-330.
- [14] Chen, G.G. and Hsu, T.R., A mixed explicit-implicit (ei) algorithm for creep stress analysis. Int. J. Num. Meth. Engng., 1988, Vol. 26, p. 511-524.
- [15] Cormeau, I.C., Numerical stability in quasi-static elasto-visco-plasticity, Int. J. Num. Meth Engng., 1975, 9, 109, p. 109-127.
- [16] Nicholson, D.W., On a stability criterion in non-associated viscoplasticity, Acta Mechanica, 1987, 69, 167-175.
- [17] Benallal, A., On the stability of some time-integration schemes in quasistatic hardening elastoviscoplasticity. Engineering Analysis, 1987, V.4, No.2, p. 95-99.
- [18] Hughes, T.J.R. and Taylor, R.L., Unconditionally stable algorithms for quasi-static elasto/viscoplastic finite element analysis, Comp. Struct., 1978, 8, 169-173.
- [19] Nayak, G.C. and Zienkiewicz, O.C., Note on the 'alpha'- constant stiffness method for the analysis of non-linear problems, Int. J. Num. Meth. Engng., 1972, 4, p. 579-582.
- [20] Zienkiewicz, O.C., Finite Element Method in Engineering Science, McGraw-Hill, London, 1977.

- [21] Irons, B. and Ahmad, S., Techniques of Finite Elements, Ellis Horwood Limited, 1980.
- [22] Perzyna, P., Fundamental problems in viscoplasticity, Advan. Appl Mech., 1966,9, 243-377.
- [23] Nicholson, D.W., A large deformation anisotropic thermoviscoplastic constitutive model, Acta Mechanica, 1985, 55, p. 69-80.
- [24] Phillips, A. and Wu, H., A theory of viscoplasticity, International Journal of Solids and Structures, 1973, 9, p. 15-30.
- [25] Drucker, D.C., and Prager, W. Soil mechanics and plastic analysis and on limit design. Quart. Appl. Math, 10, p.157-165, 1952.
- [26] Nayak, G.C., and Zienkiewicz, O.C., Elasto-plastic stress analysis. A generalization for various constitutive relations including strain softening. Int. J. Num. Meth. Engng., 1972, 5, p. 113-135.
- [27] Nayak, G.C., and Zienkiewicz, O.C., Convenient forms of stress invariants for plasticity, Proc. ASCE, J. Struct. Div., 1972, Vol. 98, ST4, p. 949-954.
- [28] Naylor, D.J., Pande, G.N., Simpson, B., and Tabb, R., Finite Elements in Geotechnical Engineering, Pineridge Press, United Kingdom, 1981.
- [29] von Mises, R. Mechanik der festen Körper im plastisch deformablen Zustand, Göttinger Nachrichten, Math.-Phys.Kl., 1913, p.582-592.
- [30] Zienkiewicz, O.C., Valliappan, S. and King, I.P., Elasto-plastic solutions of engineering problems 'initial stress', finite element approach, Int. J. Num. Meth. Eng., 1969, 1, p. 75-100.
- [31] Thomas, J.N., An improved accelerated initial stress procedure for elasto-plastic finite element analysis. Int. J. Num. Anal. Meth. Geomech., 1984, 8, p.359-379.
- [32] Brockman, R.A., Explicit forms for the tangent modulus tensor in viscoplastic stress analysis, Int. J. Num. Meth. Engng., 1984, 20, p. 315-319.
- [33] Das, B.M., Principles of Foundation Engineering, Prindle, Weber and Schmidt Publishers, 1984.

- [34] Crouch, S.L., and Starfield, A.M., Boundary Element Methods in Solid Mechanics, George Allen & Unwin (Publishers) Ltd., London, 1983.
- [35] Odqvist, F.K.G., Mathematical Theory of Creep and Creep Rupture, Oxford University Press, 1974.
- [36] Stolle, D.F.E., Finite Element Modelling of Creep and Instability of Large Ice Masses, PhD Thesis, McMaster University, Hamilton, Ontario, Canada, 1982.
- [37] De Borst, R., and Vermeer, P.A., Possibilities and limitations of finite elements for limit analysis, Geotechnique, 1984, Vol. 34, No. 2, p. 199-210.
- [38] Johnson, W., and Mellor, P.B., Engineering Plasticity, Van Nostrand Reinhold Company Limited., Berkshire, 1978.
- [39] Chen, W., Limit Analysis and Soil Plasticity, Elsevier Science Publishing Company, 1975.